THERMALLY DESTRATIFYING LAKES AGAINST BLUE ALGAE WITH RISING AIR BUBBLES

MSc thesis by Matthijs Hekstra

Delft, 2015

Faculty Civil Engineering & Geosciences

TU Delft

Faculty of Engineering

NUS

Graduation committee:

Dr Olivier Hoes (TU Delft)

Prof Dr Ir. Nick van de Giesen (TU Delft)

Drs. Bruce Michielsen (Hoogheemraadschap van Rijnland)

Dr Ir. Marcel Zijlema (TU Delft)

Dr Vivien Chua (NUS)

Date of defence:

10 December 2015

TU Delft Delft University of Technology

NUS National University of Singapore

Hoogheemraadschap van Rijnland

ABSTRACT

Mixing systems are used in deep lakes to prevent blue algae from rapidly growing. Air bubbles rise from the bed, dragging water from below upwards. The resulting vertical circulation suppresses blue algae growth. However, these systems demand electricity of about €25,000 per km^2 per year. The airlift promises to mix the water more efficiently, using a vertical tube wherein the bubbles rise.

Small-scale laboratory experiments presented in this thesis show that the airlift is slightly slower in completely removing stratification than a single bubble plume with the same air flow. 3D schematisations hereof using Delft3D are indifferent. A case study using 3D schematisations of Lake *Haarlemmermeerse Bos* also shows that the airlift is not more efficient. Hence generally the airlift is not better for lake destratification than a bubble plume system.

CONTENTS

Abstract 3

1 Introduction 6

1.1 Background 6

1.2 Hypothesis 6

1.3 Method and reading guide 6

2 Blue algae 8

2.1 General appearance 8

2.2 Nuisance 9

2.3 Growth 9

2.3.1 Biological process 9

2.3.2 Stratification 11

2.3.3 Scum 12

3 Bubble plume systems 14

3.1 Structure 14
3.2 Hydrodynamic effects 15
3.3 Ecological effects 16
4 Airlift 18
4.1 Structure 18
4.2 Effects 19
4.3 Case lake Ursem 20
4.4 Case Lake *Kotermeerstal* 22
5 Management of deep lakes by water boards 23
5.1 Historical and legal basis 23
5.1.1 EU Water Framework Directive 23
5.1.2 EU Bathing Water Directive 24
5.2 Management by water board *Rijnland* 24
5.2.1 Artifial mixing measures by *Rijnland* 26
5.2.2 Other measures against blue algae 29
6 Airlift experiment 31
6.1 Hypothesis and set-up 31
6.2 Visual Observations 31
6.2.1 Airlift 31
6.2.2 Bubble plume 32
6.3 Temperature Measurements 32
7 3D Modelling of the airlift 34
7.1 Introduction to the experiment schematisation 34

7.2 Results experiment schematisation 35

7.3 Introduction to the case study lake *Haarlemmermeerse Bos* 36

7.4 Results of the case study lake *Haarlemmermeerse Bos* 39

7.4.1 Airlift mixing 40

7.4.2 Bubble plume mixing 41

8 Conclusion and recommendations 43

References 45

Appendix A: Matlab scripts for experiment 52

Appendix B: Results lab experiment 57

Appendix C: Results Schematisation experiment 60

Appendix D: Set-up details of the Delft3D schematisations 62

D.1 Set-up details schematisation experiment with the bubble plume 62

D.2 Set-up details Schematisation experiment with the airlift 63

D.3 Set-up details Schematisation case study lake *Haarlemmermeerse Bos* 65

Appendix E: Map of Lake *Haarlemmermeerse Bos* 69

Appendix F: Calibration of case study Lake *Haarlemmermeerse Bos* 70

1 INTRODUCTION

1.1 BACKGROUND

Summer in, summer out, floating layers of blue algae are the cause of temporary closure of bathing locations in ponds and lakes and in particular the deep ones. These blue algae excrete toxins that are harmful or even lethal for flora and fauna; as well as capable of causing serious skin irritations or other complaints to people. The water boards are responsible for the water quality of these water bodies in the Netherlands and try to reduce the amount of blue algae in deep lakes by means of air-bubble mixing systems. These systems mix the temperature layers on different depths in the water; moving the blue algae to deep, dark parts of the water. The energy costs of this so-called destratification of a lake are several tens of thousands euros per year and for this reason it is desirable to explore other ways of mixing that are more efficient.

The airlift is a mixing system that – compared with a conventional 'open' mixing system – guides the bubbles through a tube from the bed to the surface. As a result, there is no exchange of water during the ascent of the bubbles, allowing a lake with an airlift to be mixed with much less energy. The airlift is the subject of the present thesis.

1.2 HYPOTHESIS

The hypothesis of this thesis is that an airlift is a much more energy efficient structure than a conventional bubble plume to destratify deep waters.

1.3 METHOD AND READING GUIDE

The first few chapters of this thesis are the result of a literature study on blue algae and measures against them. From chapter 6, this information is used to perform laboratory experiments and create 3D schematisations.

Blue algae are cyanobacteria. Chapter 2 explores this type of bacteria. It is important to know what blue algae look like and to understand in which conditions they grow and type of problems they cause in local water bodies, in order to later be able to deal with them.

Blooms of blue algae are commonly reduced by mixing systems that use rising air bubbles to force a vertical circulation in the water. Chapter 3 goes into detail of the structure of these mixing systems and their effect on the flow and ecology.

The airlift promises to do same suppression of blue algae as a conventional mixing system. Chapter 4 elaborates on the appearance of the airlift and its results against blue algae on two locations in the Netherlands.

Chapter 5 shows the European-wide coordinated laws that dictate monitoring of and action against blue algae nuisance. Water boards are responsible for the water quality in the Netherlands. Measures taken by the water board *Rijnland* (Dutch: *Hoogheemraadschap van Rijnland*) are investigated. They focus on a good water quality in general, but as long as it is needed, symptoms of an imperfect water system are engaged with the mixing systems. An overview is given of the deep lakes of water board *Rijnland*, including the mixing locations and their details.

In chapter 6, a laboratory experiment – that provided the general insight in the flow induced by the airlift as presented in chapter 4 – compares the mixing capability of an airlift with that of a single bubble plume.

The laboratory experiment serves as a guide to model both mixing system types in Delft3D, a 3D modelling suite. A model for a bubble plume is present as a Delft3D module, but an airlift model is to be invented newly. A case study is done to observe the results in a large-scale application using a 3D schematisation of Lake *Haarlemmermeerse Bos* that has four locations of bubble plumes. The results of this modelling work can be found in chapter 7.

Together, these results show a complete picture of the blue algae problems and the mixing that used against them. Chapter 8 concludes this thesis.

2 BLUE ALGAE

This chapter describes blue algae, their appearance, important factors for growth and causes for nuisance for a general public. In short, (freshwater) blue algae are bacteria that need Nitrogen, Phosphorus and light to grow. Many species are toxic. Vertical temperature differences support blue algae domination over green algae. Some blue algae species form floating layers on the surface.

2.1 GENERAL APPEARANCE

Blue algae are not a species of algae like the name suggests, but are cyanobacteria. They belong to the phytoplankton organisms, because their mechanism of photosynthesis is similar to that of algal and plant chloroplasts and they have chlorophyll-a (Silva and Moe, 2014). However, the cells do not have a nucleus (prokaryotic), whereas the cells of algae and plants do (eukaryotic) (Konopka, 2014).

Cyanobacteria are quantitatively among the most important organisms on Earth (Garcia-Pichel et al., 2003). Because of the chlorophyll, they are green. Their name is derived from the phycocyanin pigment they produce that in sufficiently high concentration is bluish. Therefore, their popular name is blue-green algae, blue-greens or simply blue algae (Schopf, 2012). In some cases the red phycoerythrin or other pigments are formed, causing the cyanobacterium to have a different colour.

Cyanobacteria appear in many different types. Not only can the colour be different. The shape ranges from unicell to filament (Lalli and Parsons, 1997). The size can be a micrometre big or 10 cm long. They can be found nearly everywhere on earth, living in the harshest environments. Their omnipresence and capability to produce oxygen, has led to the statement that this was the organism that caused Earth to progress to a life sustaining, oxygenated planet (Buick, 2008).

Cyanobacteria possess several characteristics that make them successful. The temperature optimum for most cyanobacteria is at least several degrees higher than for most eukaryotic algae (Castenholz and Waterbury, 1989). They are among the most successful organisms in highly saline environments. Forms that live on land often tolerate high levels of ultra-violet irradiation. Many planktonic forms have efficient a photosynthesis at low light conditions (Van Liere and Walsby, 1982). Sometimes photosynthetic CO_2 reduction can proceed efficiently at

very low concentrations of inorganic carbon (Pierce and Omata, 1988). Some freshwater plankton species have the ability to form gas vacuoles, hence increasing the cell buoyancy.

The more common species in freshwater are the Microsystis, Anabaena, Aphanizomenon, Lyngbya, Nodularia, Planktothrix, Nostoc and Cylindrospermopsis species (Stone and Bress, 2007).

2.2 NUISANCE

Cyanobacteria are notorious because of their capability to produce toxins. 50-75% of bloom isolates can produce toxins, often with more than one toxin being present (Skulberg et al., 1993; Yoo, 1995; Codd & Bell, 1996). The presence of high concentrations of these cyanobacteria poses a threat for humans and animals (Lurling and Faassen, 2013; Codd et al., 2005; Dittmann and Wiegand, 2006). Toxins are classified according to their mode of action into hepatotoxins (e.g. microcystins), neurotoxins (e.g. anatoxins), skin irritants, and other toxins (World Health Organization, 2003). Both hepatotoxins and neurotoxins are produced by cyanobacteria commonly found in surface water (Carmichael, 1992; Fawell et al., 1993). The more common species in freshwater are the Microsystis species, Anabaena species, Aphanizomenon species, Oscillatoria species and the Planktothrix species. Besides the toxins, a lower transparency, less dissolved oxygen and lower nutrient levels caused by cyanobacterial blooms can suppress plant growth seriously.

2.3 GROWTH

2.3.1 BIOLOGICAL PROCESS

Cyanobacteria reproduce themselves by cell division. In order to do so, they need nutrients which they extract from the water – mainly N and P – and energy. They obtain the energy needed from the chemical process of photosynthesis.

Photosynthesis takes place in the chloroplast cell body of a cell and exists of two parts: the light reaction and the dark reaction. The light reaction starts in pigments like chlorophyll. Different pigments can collect energy from different wave lengths. The energy is used to break down water (or another electron source) in oxygen and hydrogen. The oxygen is transported out of the chloroplast and the hydrogen reacts with $NADP^+$ to NADPH (reduced nicotinamide adenine dinucleotide phosphate) and with ADP and P to ATP (adenosine triphosphate).

The dark reaction is also called the Calvin cycle (Calvin, 1961). It is independent of light, but requires the hydrogen and energy stored in the NADPH and ATP from light reaction. It fixes carbon from ambient CO_2 to sugars like CH_2O. These can be combined to much more complex carbohydrates in the Calvin cycle.

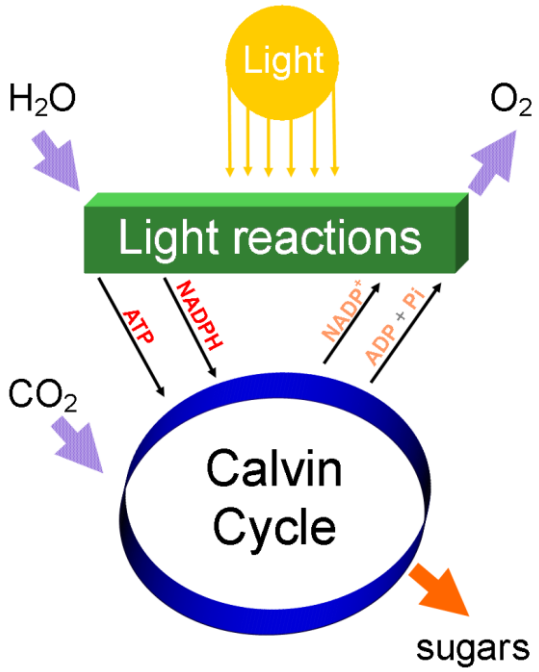


Figure 1: A simplified diagram of photosynthesis. Source: Mayer, 2008.

To summarise the two photosynthetic reactions in one chemical reaction formula (Niel, 1931):

$$H_2O + CO_2 \rightarrow CH_2O + O_2 \quad (1)$$

A chemical reaction like photosynthesis runs at a certain speed that is determined by its surroundings. Salinity is important, but in freshwater bodies is the most important factor is temperature (Verspagen et al., 2006). The relationship between growth rate and temperature is exponential. Figure 2 shows that the growth rate accelerates greatly above 20 degrees.

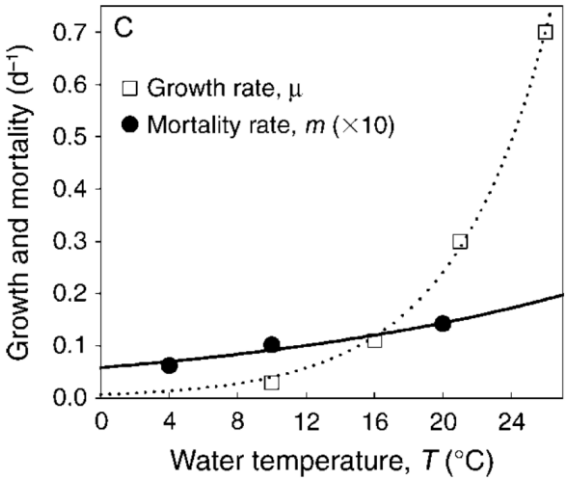


Figure 2: The specific growth rate *μ* and specific mortality rate *m* (x10) of Microsystis plotted as functions of temperature *T*. Source: Verspagen et al., 2006.

Hence, the growth of cyanobacteria is limited by the availability of light for photosynthesis, nutrients for cell division (Huisman and Hulot, 2005) and the temperature determines the speed. As long as this triangle of light, nutrients and temperature is sufficiently available, concentrations of cyanobacteria can increase greatly: a bloom. This is measured by a high level of chlorophyll and in a eutrophic lake, chlorophyll-a concentrations may reach 300 µg/L. Conditions favouring the formation of cyanobacterial blooms in lakes and reservoirs are: summer density-stratification, high water temperatures, low turbulent diffusion, high level of nutrients (eutrophication, especially Nitrogen and Phosphorus), low light extinction (clear waters), and their high resistance to grazing by zooplankton (Medrano, 2014; Paerl and Ustach, 1982; Reynolds, 1987; Shapiro, 1997). But even in the shadows of other organisms cyanobacteria grow steadily. Their maintenance constant is low, which means that they require little energy to maintain cell function and structure (Gons, 1977; Van Liere et al., 1979).

Cyanobacteria outcompete other phytoplankton also because many of them are capable of regulating their buoyancy status (Walsby and Bleything, 1988; Ibelings et al., 1991; Medrano, 2014). They control their carbohydrates content and have gas vacuoles: hollow chambers that are permeable, rigid structures of proteins that have a density of about one tenth that of water. These features cause the cyanobacteria to have a density just above or below the density of water (Walsby, 1987; Mur et al., 1990; Visser et al., 2005).

2.3.2 STRATIFICATION

The ability to regulation buoyancy is especially useful in an environment where regular vertical movement is hindered by stratification of the water column. A lake is stratified when the water

at the bottom (the hypolimnion) is colder, saltier, more saturated or – in general – denser than the water at the top (the epilimnion) (Pietrzak, 2012), see Figure 3. The transitional layer in between is called the metalimnion. The thermocline (temperature stratification) or pycnocline (in general) is the plane where the maximum rate of density decrease is with respect to the depth. The focus of this thesis is on lakes that are stratified by temperature.

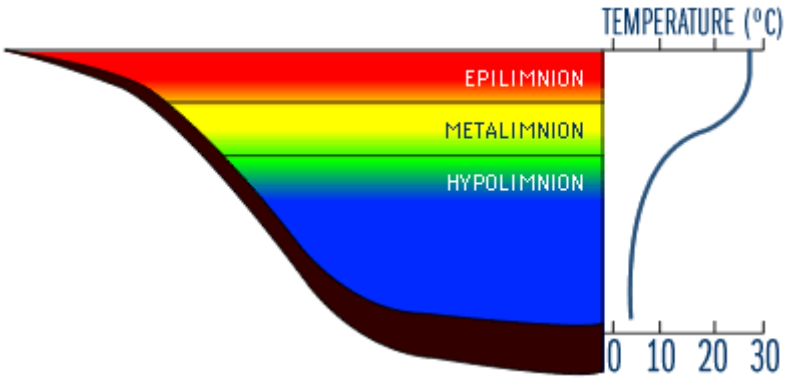


Figure 3: Temperature stratification in a lake. Source: Water on the Web, 2015.

Temperature stratification occurs in lakes under the influence of solar radiation. The heat of the sun only penetrates a certain depth, depending on the transparency of the water. This means that shallow lakes are warmed up over the entire vertical – leaving aside micro stratification (Oral communication with B. Michielsen from water board *Rijnland* in March 2015). Deeper lakes develop a stratification that is rather strong, meaning that the thermocline is thin compared to the water depth.

Phytoplankton in a lake without a thermocline is mixed through the water column by the vertical turbulence that is caused by the wind. A thermocline limits this vertical turbulence to the epilimnion (Pietrzak, 2012). Phytoplankton that is out of light's reach (the aphotic zone) does not grow (see section 2.3.1). Cyanobacteria, however, use their gas vacuole to adjust their depth to one that does give them light, ignoring the divisive thermocline. This enables them to receive an optimal amount of light during the day and nutrients during the night by migrating daily (Ibelings et al., 1991).

2.3.3 SCUM

When cyanobacteria rise to the water surface, a scum layer may be formed. Its life span is several hours to days and it looks like as if a green sheet is covering (parts of) the surface of the lake (Medrano, 2014). A bloom does not necessarily produce a scum (Zohary and Breen, 1989). The conditions required for scum formation are: the existence of a large population of

cyanobacteria, positively buoyant colonies that reach the surface of a lake and stability of the water column (stratification); complemented with the oxygen supersaturation degree in the water needed for bubble growth (Medrano, 2014). Of course only species that have this buoyancy regulation and that are suitable for possible bubble formation are candidates for forming scum. These species in general have a higher tolerance for high light intensities (Mur et al., 1990; Paerl et al., 1982).

3 BUBBLE PLUME SYSTEMS

This chapter describes bubble plume systems that are used to reduce blooms of blue algae. The system consists of several diffusors on the water bed and is powered by a generator on-shore. It brings the water in a circulation and mixes vertical differences. It suppresses blue algae growth because of a lower water temperature, increased turbulence, a downwards transportation towards the dark and oxygenation.

3.1 STRUCTURE

A bubble plume system is able to transport water in upward direction with rising air bubbles. The bubbles can be concentrated in several locations ('point aeration' with bubble plumes) or arranged in lines ('line aeration' with bubble screens). A bubble plume system is used as a method of artificial mixing of horizontal water layers, but is also used as separation measure. Near ship locks, bubble screens block horizontal flows of salt and oil spills are contained by bubble screens blocking the floating oil (Abraham et al., 1973; Kobus, 1975).

A bubble plume system is not a predefined structure. Depending on the location, its morphology and purpose, it is constructed differently. The system typically consists of multiple air diffusers, air transport pipes and a compressor that is placed on shore.

Figure 4 shows one of the point aerators in Lake *Haarlemmermeerse Bos*. The diffusers are located at the bed in the deepest parts of the water and connected through pipes to the compressor on shore that delivers to all aerators.

A system like this requires a prohibition of anchoring to avoid damaging of the tubes or pipes.



Figure 4: Diffuser in Lake *Haarlemmermeerse Bos*: point aeration by four perforated tubes (two old and two new ones). Source: Stroom and Schaik, 2007.

3.2 HYDRODYNAMIC EFFECTS

The air diffuser is designed to release air in small bubbles. The bubbles are – depending on the depth – between two and three orders more buoyant than water. They impose a drag force on the water. Next to the amount of bubbles also the size of the bubbles matters. It influences the rising speed (Lehrer, 1980; Wesselingh, 1987), the drag force (Moore, 1959) and hence the amount of entrained water. The amount of entrained water is one or two orders higher than the amount of injected air. A rising bubble plume fans out and the total width of the water that is entrained is even 20% wider (Milgram, 1983), see Figure 5.

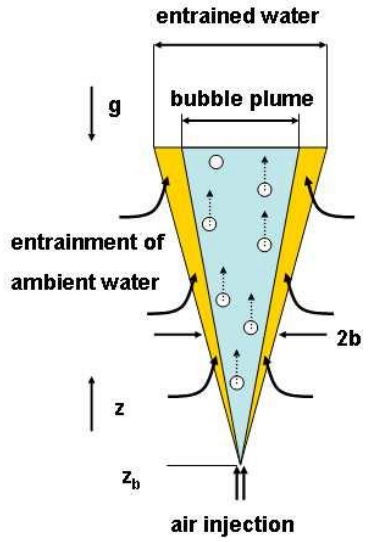


Figure 5: Schematic axisymmetric bubble plume with entrainment of water by the rising bubbles (source: Deltares, 2011 a)

The bubble plume induces vertical circulation patterns that are often based on the lateral diversion of the water entrained in a bubble plume into a horizontal flow at the surface (Deltares, 2011a). See Figure 6.

The rising bubbles drag along water and transfer their potential energy to kinetic energy of the entrained water. Upon reaching the water surface, this kinetic energy is first converted into an increase in potential energy i.e. the level of water surface increase above the rising bubble plume. Subsequently, this locally increased water level induces a horizontal, lateral current away from the vertical symmetry axis/plane of the bubble plume. This lateral current forms another jet that also entrains water from below. This secondary entrainment creates a large amplification factor compared to the injected air flow. Experiments of 2D bubble screens show that the lateral, horizontal jet initially has a thickness that is roughly 20-25% of the injection depth (see “U>0” in Figure 6). The conversion from kinetic energy into potential energy and

successively converted into horizontal flow implies that the initial momentum in the lateral jet equals the momentum of the entrained water in the rising jet.

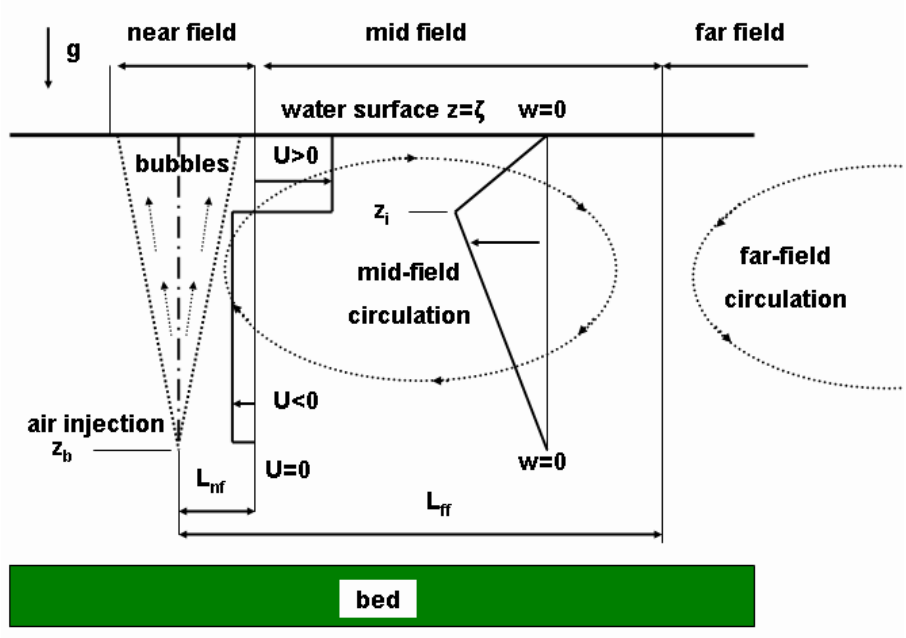


Figure 6: Definition of near-, mid- and far-field of the circulation induced by a bubble plume and the vertical profile of the vertical (downward) velocity in the mid-field circulation. (Source: Deltares, 2011a.)

3.3 ECOLOGICAL EFFECTS

The vertical circulation patterns induced by the bubble plume have several consequences. First, the horizontal temperature layers (see 2.3.2) are mixed. In other words, vertical stratification is removed. The temperature becomes uniform and lies between the temperature of the former epilimnion and hypolimnion. The euphotic zone cools down several degrees. This is the zone with sufficient light for photosynthesis (from the Greek *eu*, good, and *phoos*, light) and is roughly 1.7 times the water transparency (Scheffer, 1998). The zone below the euphotic zone is called aphotic zone.

Secondly, turbulence mixing increases because the thermocline is absent now. The mixing is assumed to be provided by wind-generated turbulence that is no longer damped by density stratification after removal of the thermocline (Deltares, 2011b). The increase of turbulence in the lake should subsequently mix phytoplankton downwards into the aphotic zone. The bigger the aphotic zone is compared to the euphotic zone, the higher the time fraction with phytoplankton remaining in darkness (Ibelings et al., 1994; Jungo et al., 1993). Also, an increase of turbulence may shift the competitive balance between buoyant and sinking phytoplankton species (Huisman et al., 2004).

Thirdly, the recirculation causes a downwards flow that drags down anything floating in the water. This includes phytoplankton that depends on the light in the euphotic zone for photosynthesis. The assumption is that the more time is spent in the aphotic zone, blue algae blooms less or not at all (Deltares, 2011b; Ibelings et al., 1994). This would demand a sufficiently strong vertical recirculation with a downward velocity that exceeds the maximum rising velocity of blue algae colonies. Again, the bigger the aphotic zone is compared to the euphotic zone, the higher the time fraction with phytoplankton remaining in darkness.

Fourthly, the lake is oxygenated. The mixing and recirculation increases the concentration of dissolved oxygen near the bed. This reduces the amount of cysts of blue algae in the bed entering the water and removes the bed as a source of blue algae (Sirenko, 1972). Also, the increased concentration of dissolved oxygen is harmful for blue algae; however, they protect themselves with mucus (Sirenko et al., 1968; Reynolds, 2007).

Finally, the lateral surface flows are important for the shallow zones surrounding a lake. They flush this water that is not included in the vertical mixing and circulation, reducing possible high concentrations of blue algae and spreading scums.

4 AIRLIFT

This chapter describes the airlift as an alternative to conventional bubble plume systems. The structure is characterised by the vertical tube through which the air bubbles rise. It brings the water in a circulation and mixes vertical differences. It suppresses blue algae growth because of a lower water temperature, increased turbulence, a downwards transportation towards the dark and oxygenation.

4.1 STRUCTURE

The airlift is a vertical plastic tube wherein air bubbles rise. The tube is hanging under a float, see Figure 7 and Figure 8. The top of the tube is at the water level and the bottom some distance above the bottom of the lake. A compressor on the float pumps air from the surface to a diffusor that make small bubbles. The bubble plumes are released underneath the tube.

There are at least two cables needed to anchor the tube to a fixed position. A hose is transporting air from the surface to below. Electricity needs to be provided. Alternatively, one could choose to locate the compressor on-shore.

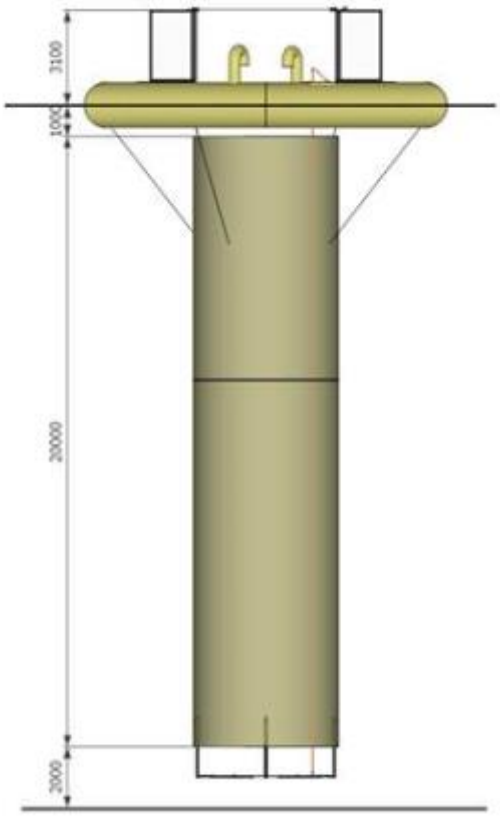


Figure 7: schematic representation of the airlift (side view). Source: FishFlow Innovations.



Figure 8: The airlift in Lake *Ursem* (see section 4.3. Source: Molenaar, date unknown) and in the Lake *Kotermeerstal* (see section 4.4. Source: FishFlow Innovations, 2013).

4.2 EFFECTS

The airlift functions as a giant pump that transports water vertically from bottom to top. The air bubbles induce drag forces on the water while they rise, dragging along the water. This causes water to flow upwards through the tube. The rising water does not interacting with the water around the airlift. Only after the water is virtually teleported upwards, the flow spreads horizontally, mixing the epilimnion. (See also section 6.2.1 and 6.3 for a description based on the experiment.)

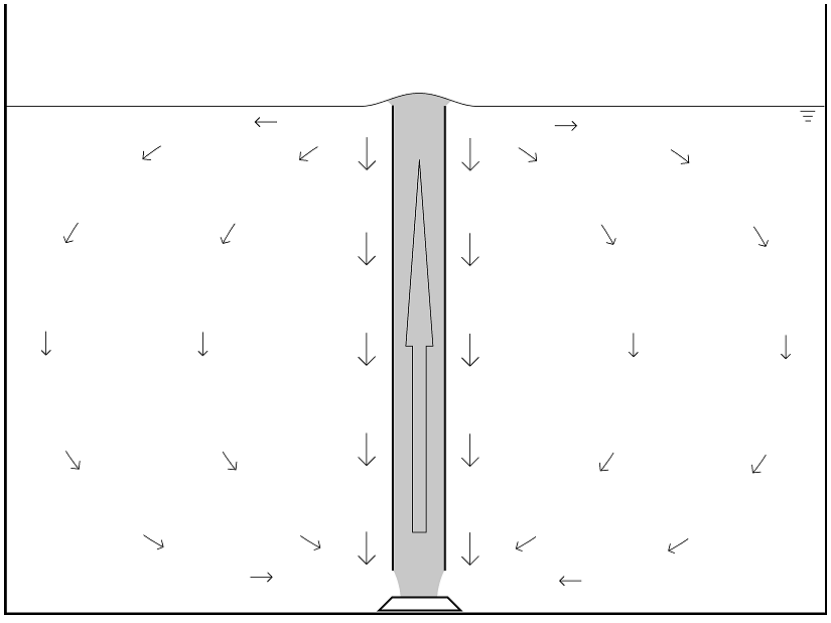


Figure 9: Sketch of the observed flow during the experiment with an airlift.

The manufacturer sells the airlift as an alternative for a conventional bubble plume system with lower costs, both in operation (FishFlow Innovations, date unknown) as in construction (oral communication with G. Manshanden from FishFlow Innovations in March 2015). This is

possible because the airlift ensures that the mixing of water happens over the maximum vertical distance possible: from the bottom to the top of the lake. The deeper, cold and nutrient-poor parts of a lake are mixed with the higher, warm and nutrient-rich water. Also, the amount of dissolved oxygen is increased in the lake due to the circulation in the lake, which harms blue algae (Sirenko et al., 1968).

4.3 CASE LAKE URSEM

In 2011, the airlift was built for *Recreatieschap Westfriesland* in Lake *Ursem* (see Figure 10, Dutch: *Ursemmerplas*) to show that blue algae problems can be fought for a much lower financial cost than conventional mixing with air (FishFlow Innovations, 2011). Lake *Ursem* is a 30 ha big lake with a maximum depth of 15 m and an official swimming location. Swimming prohibitions due to blue algae blooms were active for weeks every summer.



Figure 10: Location Lake *Ursem* and Lake *Kotermeerstal* in the Netherlands (licensed under Creative Commons).

The reason that an airlift is cheaper than traditional bubble plume mixing installations is mainly because of a smaller construction size and a smaller compressor. Table 1 shows the specifications of the airlift in Lake *Ursem*. To put these numbers into perspective, the Lake *Nieuwe Meer* system is given as reference, as well as a hypothetical airlift in Lake *Nieuwe Meer* as calculated by Arcadis (Arcadis, 2014).

Table 1: Comparison between the current airlift system in Lake *Ursem* and a proposed one in Lake *Nieuwe Meer*. The current line aeration system in Lake *Nieuwe Meer* is given as reference. It shows the enormous difference between the compressor and the resulting flow used for the airlift and line aeration system.

Lake	*Lake Ursem (airlift)*	*Nieuwe Meer (current)*	*Nieuwe Meer (airlift)*
Area	$0.3*10^6$ m^2	$1.3*10^6$ m^2	$1.3*10^6$ m^2
Volume	$2*10^6$ m^3	$18*10^6$ m^3	$18*10^6$ m^3
System type	Airlift (1)	7 lines	Airlifts (3)
Alga control principle	Non-stagnancy and aeration	Circulation	Non-stagnancy and aeration
Air flow		260 l/s	41.7 l/s
Water flow	1.5 m^3/s	585 m^3/s	4.5 m^3/s
Downward velocity	0.005 mm/s or 0.4 m/day	4.5 mm/s or 39 m/day	0.0003 mm/s or 0.3 m/day
Circulation time	15.4 days	0.3 days	46.3 days
Construction	€200k	€1200k	€600k
Energy yr^{-1} calculated	€1.1k	€32k / €60k	€11k
Energy yr^{-1} km^{-2}	€3.7k	€25k / €46k	€8.4k
Compressor	3 kW	50 kW + 37 kW	3x 2x 5 kW
Water flow per kW	0.5 $m^3/s/kW$	6.7 $m^3/s/kW$	0.5 $m^3/s/kW$
Blooms / scums	High bio mass and scums sometimes	None	Not applicable

The table shows that the airlift uses much less power, but is also less efficient in transporting water. Based on these statistics, water company *Waternet* (Amsterdam) views the airlift as unproven in its Beating the Blues approach (Waternet, 2013a; Waternet, 2013b).

In 2012, the first complete year that the airlift was in operation, the lake remained open and only closed for a day (Buiter, 2013; Buiter et al., 2013). The wind was absent and in shallow corners scum formed. In 2013, the lake was open for bathing all year. This case with an airlift in lake *Ursem* has shown that for considerably less energy (and money), the airlift could help postponing scums.

Local water board *Hollands Noorderkwartier* did not participate in this experiment, because it did not expect the airlift to work (e-mail communication with Marcel Boomgaard, *Hollands Noorderkwartier*). Also after two years of experience with the airlift in Lake *Ursem*, the water board states that the technique has not been proven to work. Measurements of chlorophyll levels – a measure of the amount of algae – keep showing high levels of bio mass. And in 2014 and 2015, scum layers returned (RTV NH, 2014; RTV NH, 2015).

4.4 CASE LAKE *KOTERMEERSTAL*

In 2013, an airlift was built in Lake *Kotermeerstal* for the Dutch municipality *Hardenberg* (FishFlow Innovations, 2013). Lake *Kotermeerstal* (see Figure 10) has a size of 12 ha and has a maximum depth of 8 m, although most of the lake is only 1-2 m deep. The lake is isolated and only fed by rain and seepage. After the results of this airlift were insufficient in 2014, the experiment was stopped (De Toren, 2014).

5 MANAGEMENT OF DEEP LAKES BY WATER BOARDS

This chapter describes the role of water boards and legislation that also targets blue algae. Measures taken against blue algae taken by water board *Rijnland* are taken as an example, because they use mixing systems in four different lakes.

5.1 HISTORICAL AND LEGAL BASIS

Alongside three layers of general-purpose government bodies, national, provincial and municipal, there are water boards with the sole task of managing water. The national Water Law (2009) shows the organisation of water management (Invoeringswet Waterwet, 2015; Waterwet; 2015). Except for the large water bodies like major rivers and the sea, the water boards are responsible for the management of all regional surface water bodies and their embankments. The boards' fundamental task has since the first mention of the existence of water boards in 1255 been to protect the country from flooding (Hoogheemraadschap van Rijnland, date unknown-a). Since 1970, when the Pollution of Surface Waters Act came into force, the water boards are also responsible for water quality (Wet Verontreiniging Oppervlaktewateren, 2015). The in 2000 issued EU Water Framework Directive aims to organise a good quality status for ground and surface waters internationally (EU Water Framework Directive, 2000). Finally, the EU Bathing Water Directive from 2006 protects the health of bathers (EU Bathing Water Directive, 2006).

5.1.1 EU WATER FRAMEWORK DIRECTIVE

Since the rise of water quality laws in European countries in the seventies, the policies had been fragmented. The EU Water Framework Directive (WFD) was born to expand the scope of water protection to all waters, surface waters and groundwater. The management is based on entire river basins, like the Rhine that links Switzerland, France, Germany and the Netherlands. The approach is to have co-ordinated emission limit values and quality and combines measures with new developments. To drive all innovations, pricing of water consumption should reflect the true costs of all measures to move to clean water. There is a clear goal to achieve a 'good status' for all waters by 2015, although there is a widely used possibility for a phased implementation (Hoogheemraadschap van Rijnland, 2014). The Netherlands plans to reach this goal in three six-year phases (2010-2027). The various water authorities (the national Directorate-General for Public Works and Water Management (*Rijkswaterstaat*) and local water boards) all have their own policy and targets (see section 5.2 for water board *Rijnland*'s).

5.1.2 EU BATHING WATER DIRECTIVE

Problems with blue algae occur worldwide. EU-wide blue algae are monitored in the context of the European Bathing Water Directive (BWD). It requires member states to monitor any surface water location where a large number of people is expected to bathe. Monitoring is done by testing water samples during the bathing season (in the Netherlands from 1 May until 1 Oct) on intestinal enterococci and E.coli bacteria, which are measures for (faecal) pollution. Bathing water profiles inform the public about the bathing water quality and management (Interprovinciaal Overleg et al., 2015; European Environment Agency, 2014).

A bloom or scum of blue algae (see section 2.2) has its own article in the directive. Article 8: "When the bathing water profile indicates a potential for cyanobacterial proliferation, appropriate monitoring shall be carried out and adequate management measures shall be taken immediately" (EU Bathing Water Directive, 2006). However, since it is not required to test the water samples for blue algae or its toxins regularly, countries deal with these differently (Chorus, 2012). Some mainly rely on visual inspections, but in general are those supplemented by regular or incidental measurements of the number of cyanobacteria, their biovolume, the concentration of (cyano) chlorophyll-a and/or the concentrations of microcystins. In the Netherlands, the relevant water manager (either the Directorate-General for Public Works and Water Management (Dutch: *Rijkswaterstaat*) or a water board) follows the blue algae protocol (Dutch: *blauwalgenprotocol*; Nationaal Wateroverleg, 2012).

5.2 MANAGEMENT BY WATER BOARD *RIJNLAND*

The management by water board *Rijnland* covers an area of 1100 km^2 with 1.3 million inhabitants in the west of the Netherlands. *Rijnland* is responsible for the water quantity and quality management of 11,000 km of waterways (Hoogheemraadschap van Rijnland, 2015), see Figure 11. There are approximately 200 polders surrounding by dikes and with their own water level. This is possible due to 2200 weirs and four major pumping stations, discharging on average 156 m^3/s to the sea, the North Sea Channel and river *Hollandsche IJssel*. The water board also takes care of 29 wastewater treatment plants, all with the motto: "Dry feet, clean water" (Hoogheemraadschap van Rijnland, date unknown-c).

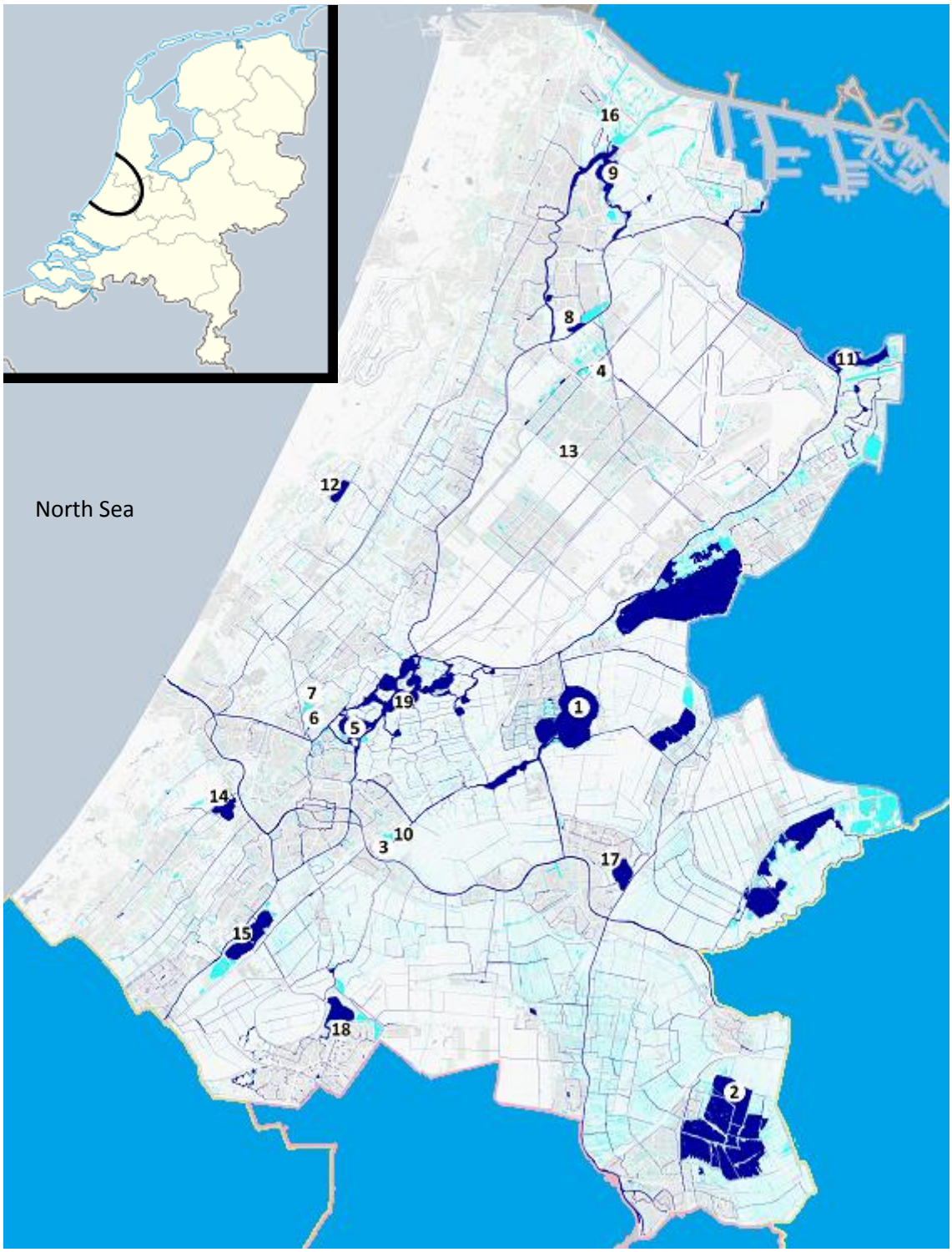


Figure 11: Rijnland on the map. Legend: main water system (dark blue), polder water (light blue), neighbouring water boards (bright blue). Deep lakes are indicated with a number (see Table 2). Map source: Rijnland, date unknown-b.

The water quality management of deep lakes is outlined in the regulation 'Policy deep pits' (Dutch: *Beleid diepe putten*; Hoogheemraadschap van Rijnland, 2000). These lakes are ecologically different from shallow waters because of wind, solar and flow effects that are

either spread over more water or split up due to the greater depth. The regulation was designed to give direction to tasks arising from the EU Water Framework Directive and the EU Bathing Water Directive.

Water board *Rijnland* pursues to deliver WFD compliant water system with water of good chemical and ecological quality and diversity. The target conditions – judged by the STOWA assessment system (STOWA, 1993) – for lakes are a long residence time (order of years), maintaining the great depth, creating ecological bank zones (wide, shallow zones) and a good chemical composition. But, while shallow systems respond with a changed equilibrium after restoration works, deep systems respond at most very slowly or not at all (Michielsen and Ibelings, 2002).

15 of *Rijnland*'s 19 deep lakes have one or two official bathing locations. Many lakes were dug for sand mining and are recreational areas now (Michielsen, 2002). At these locations, fighting symptoms like cyanobacteria for the safety of bathers is needed, since all of them – nutrient-rich or not – show a certain degree of blooms or scum (Michielsen et al., 2002).

5.2.1 ARTIFIAL MIXING MEASURES BY *RIJNLAND*

Table 2 shows an overview of *Rijnland*'s deep lakes. Fighting blue algae with bubble plume systems is currently done in lakes that had the most nuisances and bathing prohibitions. These are also lakes that are deeper than 15 metres and have very steep slopes (>1:10).

Table 2: A list of water board *Rijnland*'s deep lakes and characteristics about their shape, location and use. Their location is shown on the map in Figure 11. Lake *Klinkenbergerplas (klein)* and Lake *Munnikenpolder* are in redevelopment. 'Partial mine' means that the sand mine does not cover the entire lake. Source: Hoogheemraadschap van Rijnland, 2000.

#	Name	Max. Depth	Avg. Depth	Slope of bank	Water system	Bathing location	Bubble plume mixing
1	*Braassemmer-meer*	23	4	1:30 partial mine	Main	-	-
2	*Broekvelden Vettebroek*	32	14	1:8-100	Polder	-	-
3	*Doeshaven*	13	6	1:4	Main	-	-
4	*Haarlemmer-meerse Bosplas*	21	11	1:3-20	Polder	Yes	Yes
5	*'t Joppe*	42	13	1:6-10 partial mine	Main	Yes	-
6	*Klinkenberger-plas (groot)*	35	19	Steep	Polder	Yes	-
7	*Klinkenberger-plas (klein*	-	-	-	-	-	-
8	*Molenplas*	12	6	1:6-12	Main	Yes	-
9	*Mooie Nel*	20	5	1:6-25 partial mine	Main	Yes	-
10	*Munniken-polder*	-	-	-	-	-	-
11	*Nieuwe Meer*	31	15	1:5-10	Main	Yes	Yes
12	*Oosterduinse Meer*	15	7	1:10	Main	Yes	-
13	*Toolenburger-plas*	30	25	Steep	Polder	Yes	-
14	*Valkenburgse Meer*	36	7.5	?	Main	Yes	-
15	*Vlietlanden*	35	?	Steep	Main	Yes	Yes
16	*Westbroekplas*	30	?	?	Polder	Yes	-
17	*Zegerplas*	34	18	1:6-10	Main	Yes	Yes
18	*Zoetermeerse-plas*	30	18	Steep	Polder	Yes	-
19	*Zweiland*	18	?	Partial mine	Main	Yes	-

For the choice of the bubble plume systems, not all of the principles of artificial mixing (see section 3.3) have been considered essential against blue algae blooms. The recirculation principle was applied to the systems in Lake *Nieuwe Meer* and Lake *Zeger* (Dutch: *Zegerplas)*, see Table 3. The mixing principle was considered to be sufficient for Lake *Haarlemmermeerse Bos* and Lake *Vlietlanden*. For the latter, a schematisation in the software suite of Delft3D by Deltares Research Institute (Deltares, Date unknown) was made modelling the mixing by the bubble plumes.

Table 3: *Rijnland*'s lakes with a bubble plume system installed. The chosen type of algae control is of influence to the flow properties of the system and costs accordingly. The cost of the energy per year is noted as a calculated value and an estimated value by *Rijnland*. The calculated value is the power of the compressor multiplied by the time it is on (1 May – 1 Oct) and €0.10 per kWh. Some values for Lake *Zeger* are estimates filled in, because the design is based on the same downward velocity as in Lake *Nieuwe Meer*. Sources: Stroom et al., 2007; Deltares, 2011b; Oosterbaan and Heuzen, 2011.

Lake	*Nieuwe Meer*	*Haarlemmermeer-se Bosplas*	*Vlietland*	*Zegerplas (excl. ring)*
Area	$1.3*10^6$ m^2	$0.25*10^6$ m^2	$0.9*10^6$ m^2	$0.7*10^6$ m^2
Volume	$18*10^6$ m^3	$2.7*10^6$ m^3	$14*10^6$ m^3	~$10*10^6$ m^3
Max. depth	31 m	21 m	35 m	34 m
System type	7 lines	4 points	2 lines	4 lines
Design principle	Circulation	Mixing	Mixing	Circulation
Air flow	260 l/s	104 l/s	50 l/s	111 l/s
Water flow	585 m^3/s	13.8 m^3/s	36 m^3/s	~315 m^3/s
Air/water ratio	$4.44*10^{-4}$	$7.54*10^{-3}$	$1.39*10^{-3}$	~$3.5*10^{-4}$
Downward velocity	0.45 mm/s or 39 m/day	0.055 mm/s or 4.7 m/day	0.040 mm/s or 3.5 m/day	~0.45 mm/s or 39 m/day
Circulation time	0.3 days	2.2 days	4.4 days	~0.3 days
Construction date	1993	1999	2008	2008
Construction costs	€1200k	€480k	€550k	€550k
Energy yr^{-1}	€32k / €60k	€18k / €27	€8k / €11k	€16k / €22k
Energy yr^{-1} km^{-2}	€25k / €46k	€72k / €108	€9k / €12k	€23k / €32k
Compressor	50 kW + 37 kW	50 kW	22 kW	2x 22 kW
Blooms/scums	None	High bio mass and scums sometimes	High bio mass and scums sometimes	None

Unfortunately, even with the bubble plume systems installed, blooms and scums occur sometimes. Table 3 compares Rijnland's lakes where mixing against cyanobacterial blooms is applied. The system in Lake *Haarlemmermeerse Bos* did not significantly reduce the blue algae biovolume and did not always completely break down the stratification. Scums kept appearing every few years. The system in Lake *Vlietlanden* also did not reduce blue algae blooms, even though the stratification was successfully broken. These systems are quite a contrast with the

systems in Lake *Nieuwe Meer* and Lake *Zeger* (the latter even partly shut-down); they function very well and suppress both the bio mass and the scums.

The fact that the two bubble plume systems that were designed with the recirculation principle to control blue algae blooms are a success suggests that this is the best design principle. As a result, it also seems that the mixing principle is not. Huismand et al. (2004) presents results of a minimum amount of turbulence needed to suppress blue algae blooms. Deltares does not want to reject the mixing principle as a sufficient principle because of these results (Deltares, 2011b). It seems that the recirculation principle ensures sufficient turbulent mixing, but less turbulence might be sufficient as well. This is subject of ongoing research.

Another interesting fact rises from Table 3 when investigating the air flow to water flow ratios of the systems. The systems in Lake *Nieuwe Meer* and Lake *Zeger* have a similar (estimated) ratio, which is not surprising given the fact that they are based on the same design principle. However, the systems in Lake *Haarlemmermeerse Bos* and Lake *Vlietlanden* are also based on the same design principle and their ratios show a difference of a factor 5.4. The reason for this difference should be found in either their difference in morphology (Stroom et al., 2007) or the type of diffuser.

5.2.2 OTHER MEASURES AGAINST BLUE ALGAE

Water board *Rijnland*'s strategy in clean water is the view on the whole ecosystem (see section 5.2). In the context of blue algae this means that the chemical and biological environment is unbalanced. On locations blooms and scums occur, blue algae have plenty of nutrients to grow on, good conditions to be winning the competition with other phytoplankton (see section 2.2) and no natural enemy.

Rijnland approaches these factors integrally. The *Waternet* Beating the Blues approach (STOWA, date unknown) aims to not only do measures, but to understand the system with custom work. It splits up the problem in smaller pieces and uses preventive and curative measures. It tries to take away all sources of nutrients on which the blue algae feed. There are numerous ways to do so, like reducing nutrient-rich inflows, removing nutrient buffers and increasing nutrient outflow (flushing), see Table 4.

Table 4: Measures on system level against blue algae. Source: Waternet, 2013a.

Prevent surface flow from roads and disconnected terrains
Stop inlet nutrient-rich water or choose an alternative water inlet
Prevent incorrect connection at disconnected neighbourhoods
Flush with nutrient-poorer water
Dredge sludge that recharges the water with nutrients
Restore species balance, add more water plants and stop favouring some fish species
Disconnecting rain water, decrease nutrient inflow
Not feeding water birds/fish, decrease nutrients from excrements

Unfortunately, these measures on system level are not sufficient to suppress blue algae blooms in the discussed lakes above. Several control measure have been applied as well, but not every measure is as effective as the other and every measure comes with its disadvantages. Mixing with a bubble plume is a control measure for example. The main disadvantage of mixing with bubble plumes is that it costs €500k-€1M to construct a system and €10k-€60k per year for electricity. The production of this energy is not only counteracting the environment on a larger scale, but it also does not take away the source of the problem.

Other measures are flushing with horizontal jets to refresh shallow water and/or remove scums; removing flocks and phosphorus from the water and bottom with aluminium chloride, iron salts or iron chloride. It is also possible to attack blue algae directly by damaging the cells with hydrogen peroxide or forcing them to settle with poly aluminium chloride. The main disadvantage with the addition of chemicals to the water is that it disturbs the chemical balance in the water and sometimes harms parts of the ecosystem, flora or fauna.

6 AIRLIFT EXPERIMENT

This chapter is about a laboratory experiment that had two goals. To identify the flow patterns caused by the airlift and a single bubble plume and to test which is a faster mixer. The results were that the flow patterns were quite different, but the amount of time needed for full mixing was similar.

6.1 HYPOTHESIS AND SET-UP

The hypothesis was that the impermeable tube blocks all interacting between the vertical flow in the tube and the surrounding water, reducing the location of turbulent mixing to the epilimnion. Mixing with an airlift would be optimal if the colder water from below mixes with the warmer top layer without horizontal differences occurring. A downwards vertical flow next to the airlift was probable; even though the horizontal mixing occurs at much higher rates than vertical mixing, the mixing volume near the outflow is too small.

The experiment featured a 2.5 m long, 2.5 m wide and little over 1.5 m high tank, a diffuser existing of eight 1 mm nozzles in a row and an airlift made of a 0.2 m acrylic glass tube with the top at water level. The temperature was measured using a fibre-optic cable with a spatial resolution of 5 mm and a temporal resolution of 5 s. The stratification existed of 1.25 m of cold water (T = 15 °C) and 0.25 m warm water (T = 20 °C). The resulting density difference is the same as in a lake that warms up in spring from 4 °C (the maximum density of water) to 15°C, i.e. 0.09%. A larger difference was not possible to create, but that would only influence the final temperature. The airflow was a constant 0.28 l/s.

6.2 VISUAL OBSERVATIONS

6.2.1 AIRLIFT

The flow of the water is initiated by the rising bubbles. The bubbles exercise a frictional force on the water, dragging it along in the vertical. The bubbles' speed is influenced by their size and clustering. Bigger bubbles rise faster and a bubble train also rises significantly faster, see also section 3.2.

The bubbles are not hindered by the temperature stratification; the buoyancy is lower than both water layers. Directly above the airlift, where the bubbles leave the water, the water level

is pushed upwards a few centimetres. The water at this location is measured to have the same low temperature as in the hypolimnion.

Here, at the top, the water flows out horizontally and returns downwards without visible eddies. It is almost like the water moves downwards like a complete horizontal disc, although there are some higher flows near the walls and especially alongside the airlift itself. Because the inlet of the airlift is small compared with the flow that is going through, the accelerations towards the airlift are clearly visible. See Figure 12.

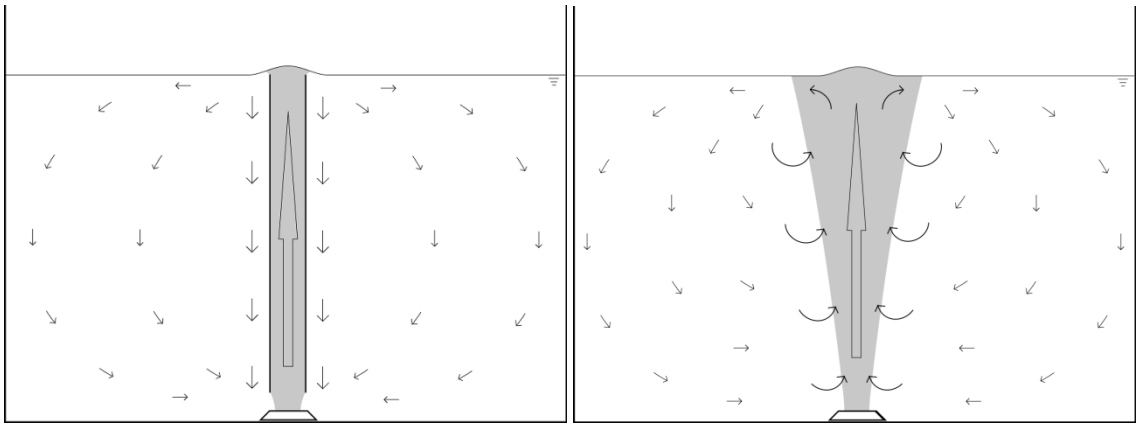


Figure 12: Sketches of the observed flow during the experiment with an airlift (left) and a bubble plume (right).

6.2.2 BUBBLE PLUME

At first view the flow that is caused by the bubble plume is not so different from the flow caused by the airlift. However, while all turbulent mixing seems to be confined in the airlift, this boundary is not present here, so there are many vortex structures surrounding the plume.

At the water level, the water remains turbulent and there is a radial flow. The water then returns to a point in the vertical (not necessarily the bottom), where it is captured in the turbulence. The flow can be described as a double-spiral motion with important secondary circulations.

6.3 TEMPERATURE MEASUREMENTS

The experiment shows small difference in time to fully mix the vertical differences in temperature between an airlift and a bubble plume. The airlift needs about eight minutes, while the bubble plume needs about seven. For both mixing systems, the depth of the epilimnion increases in time, however, the way this happens differs a lot, see Figure 13. It seems like the airlift pumps up cold water that mixes with the epilimnion without breaking the

thermocline. This amount of cold water at the surface is clearly visible in Figure 13 at t = 4 min. After the entire hypolimnion is added to the epilimnion, the mixing is complete. The bubble plume, though, seems to mix the water along the full vertical. The last local heat accumulations probably spread and take longer to completely mix. See Appendix B: Results lab experiment for all measurement results.

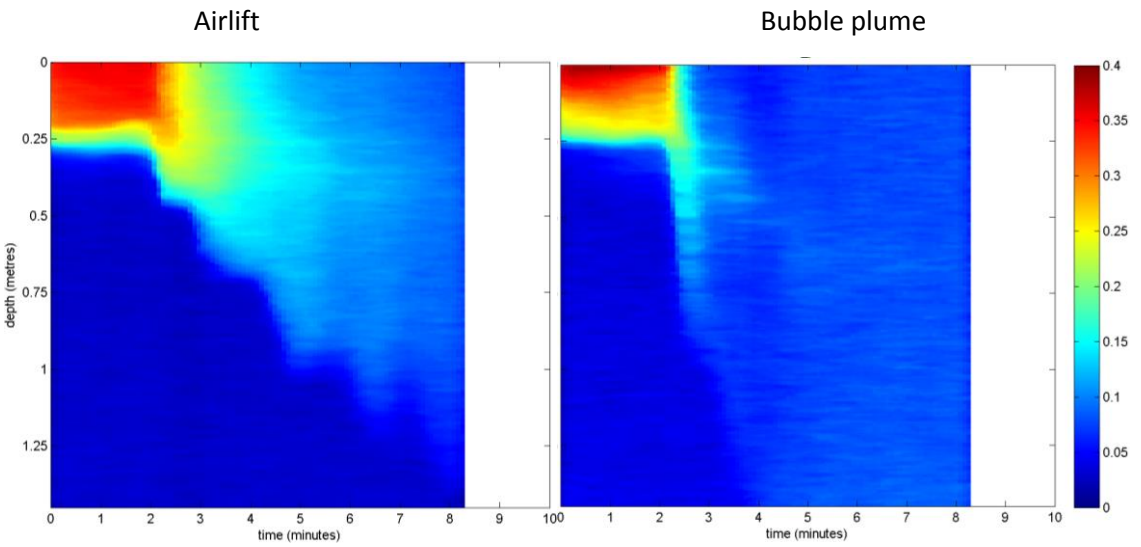


Figure 13: Temperature in space and time during the laboratory experiment. Left: airlift. Right: bubble plume. The temperature is presented as a ratio of the hypolimnion starting temperature added to the hypolimnion starting temperature. 0.4 means that the temperature is 40% higher than the hypolimnion in the beginning. The Matlab script used to convert the raw measurement data and to produce these images can be found in Appendix A: Matlab scripts for experiment.

7 3D MODELLING OF THE AIRLIFT

This chapter describes the 3D modelling of the airlift. Schematisations were made of the laboratory experiments and a case study of Lake *Haarlemmermeerse Bos*. A way to model the airlift is proposed. The outcome is that both the airlift and the single bubble plume from the laboratory results can be reproduced in the 3D schematisation, although the small difference in time to fully mix that was visible in the lab is not visible in the schematisation. The case study shows the major impact of mixing on the vertical temperature distribution in a lake, but also the very small difference between the airlift and bubble plume mixing systems.

7.1 INTRODUCTION TO THE EXPERIMENT SCHEMATISATION

Bubble plumes are already being modelled in the Delft3D software suite. There is a module that represents the flow and mixing of a bubble plume in stagnant, stratified waters and in flow. The model is based on a double plume model of a bubble core with the outer part laterally spreading out at certain levels (Mcdougall, 1978), characteristic distances of influence (Asaeda and Imberger, 1993), a relationship between the local plume properties and the mean flow properties (Milgram, 1983), and the relationship between the plume's radius and velocity and the radial flow (Fannelop and Sjoen, 1980). It was used for the bubble plume system in Lake *Vlietlanden* (see section 5.2.1). However, a comparable module for the airlift has not been developed yet.

This chapter proposes a model for the airlift and shows a Delft3D schematisation of the laboratory experiment with both airlift and bubble plume.

Section 4.2 shows the effects of the airlift on the flow. Basically, water is taken in at bed level and released at surface level without interaction with the water in between. For the model, an in-outflow construction is used that models exactly this: the water flows into the airlift at bed level, represented by an outtake in the model; and the water flows leaves the airlift at surface level, represented by an inlet in the model. The flow inside the airlift is not modelled; this is considered to be an instantaneous event.

However, any inflow would produce a vertical jet because of the hydrostatic assumption in Delft3D. In order to prevent this short circuitry, the bathymetry is edited to feature a column or tower underneath the inflow location.

The bubble plume module calculates the effects on the water on sub-grid level (Deltares, 2011a). This means that the redistributing flow is not included in the hydrodynamic results.

However, its effect on the redistribution of heat is. The input of air starts a calculation of the vertical velocity in the background. From this, a system of sources and sinks transports water and heat (see Figure 14) and because there is no water added physically, the net vertical source distribution is zero.

The model details can be found in Appendix D.

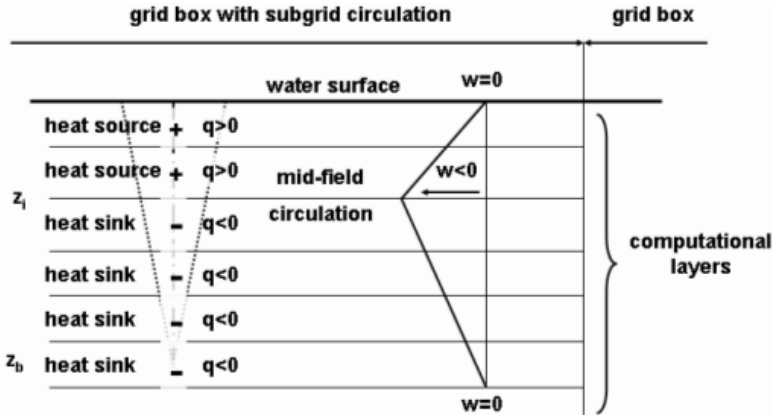


Figure 14: The bubble plume module in Delft3D. The mid field averaged heat equation with vertical distribution of sources and sinks and vertical (downward) velocity profile in a single grid box. Source: (Deltares, 2011a)

7.2 RESULTS EXPERIMENT SCHEMATISATION

As said, the schematisation with the bubble plume hardly shows flow velocities, because of the way its model was programmed. The airlift schematisation shows a stationary situation directly. The temperature profiles are used to calibrate the relationship between the air flow and the induced water flow; the latter, the so-called flux of entrained water is the input of both models:

$$Q_{ent} = (\alpha Q_{air})^{0.66}$$

Using an α factor of 27.5, the results of the schematisation approach the results from the lab experiment, as shown in Figure 15 and Figure 16. The bubble plume schematisation takes 4.5 min to become well-mixed, whereas the airlift needs 8 min, nearly double. Being well-mixed is defined the same as in the experiment: the system should not be visibly stratified; hence the maximum temperature difference is five percent.

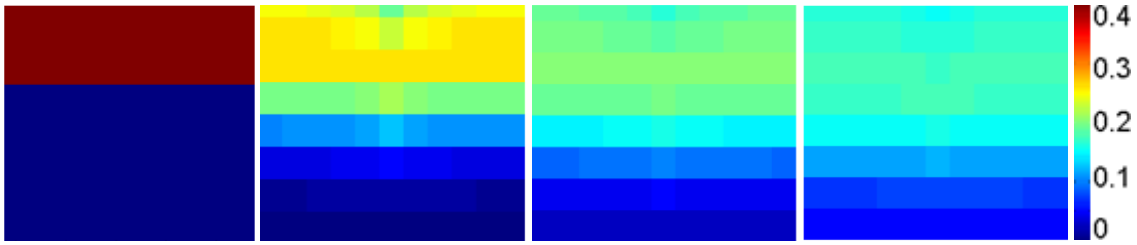


Figure 15: Temperature profiles in vertical cross-section of the experiment schematisation with the bubble plume. The temperature is relative to the starting temperature in the hypolimnion. The four frames show the temperature after 0, 1, 2 and 3 minutes.

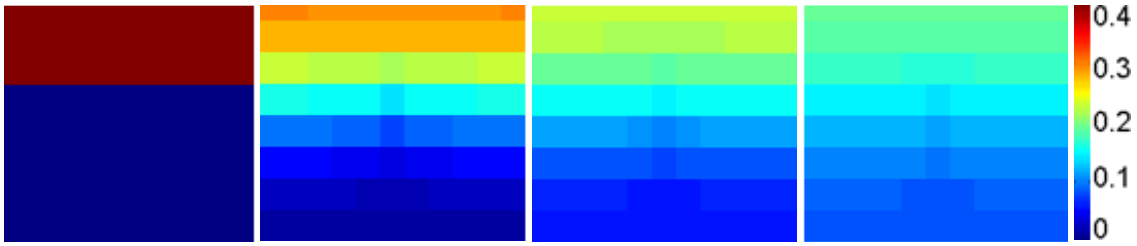


Figure 16: Temperature profiles in vertical cross-section of the experiment schematisation with the airlift. The temperature is relative to the starting temperature in the hypolimnion. The four frames show the temperature after 0, 2, 4 and 6 minutes.

7.3 INTRODUCTION TO THE CASE STUDY LAKE *HAARLEMMERMEERSE BOS*

The results from the airlift's experimental set-up and its schematisation are further examined in a case study of one of the deep lakes managed by the water board of *Rijnland*, Lake *Haarlemmermeerse Bos* (Dutch: *Haarlemmermeerse Bosplas*), which is lake number 4 in section 5.2, Figure 11 and Table 2. The bathymetry is shown in Figure 17.

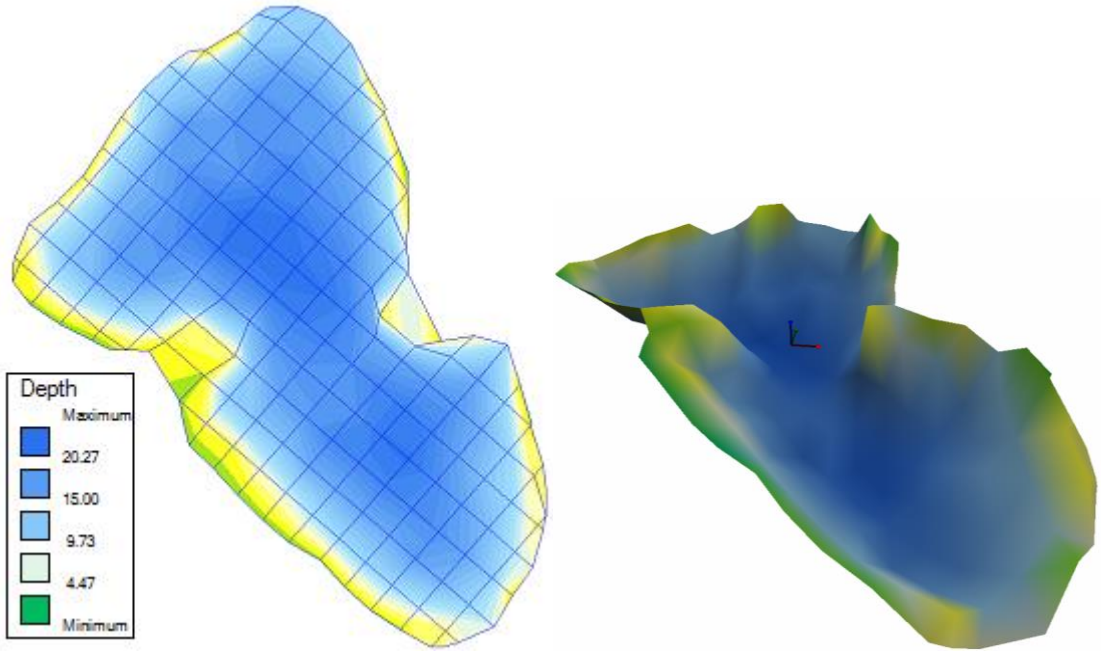


Figure 17: Bathymetry Lake *Haarlemmermeerse Bos* in 2D and 3D.

This lake has known artificial mixing since 1999 and the system is at its end of life, so the water board is considering a new system to be installed. This is possible one of a different type than the current four point aerators. In 2013, the system was thought to be old and redundant in the prevention against blue algae and the lake was thermally stratified, see Figure 18, which is a big difference compared to the mixed situation in 2012, see Figure 19. Apart from the good year of 2013, the lake needed its mixing system for the suppression of appearing blue algae blooms in the summer of 2014 again. Also in 2015, mixing was done preventive.

A detailed overview of the schematisation set-up can be found in Appendix D: Set-up details of the Delft3D schematisations. Appendix E: Map of Lake *Haarlemmermeerse Bos* shows the location of the measurement location and the cross-section that are used to present the results.

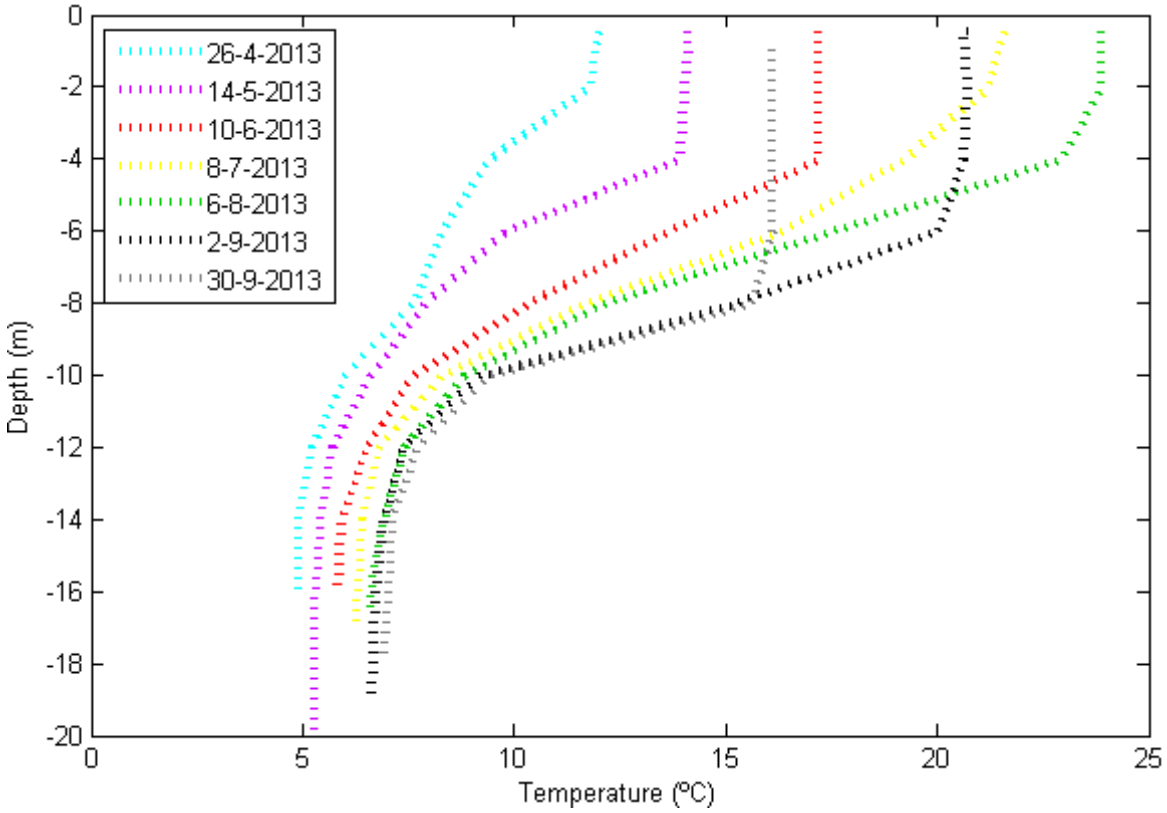


Figure 18: Temperature measurements Lake *Haarlemmermeerse Bos* from 2013. The various lines are different moments of measurement (every four weeks).

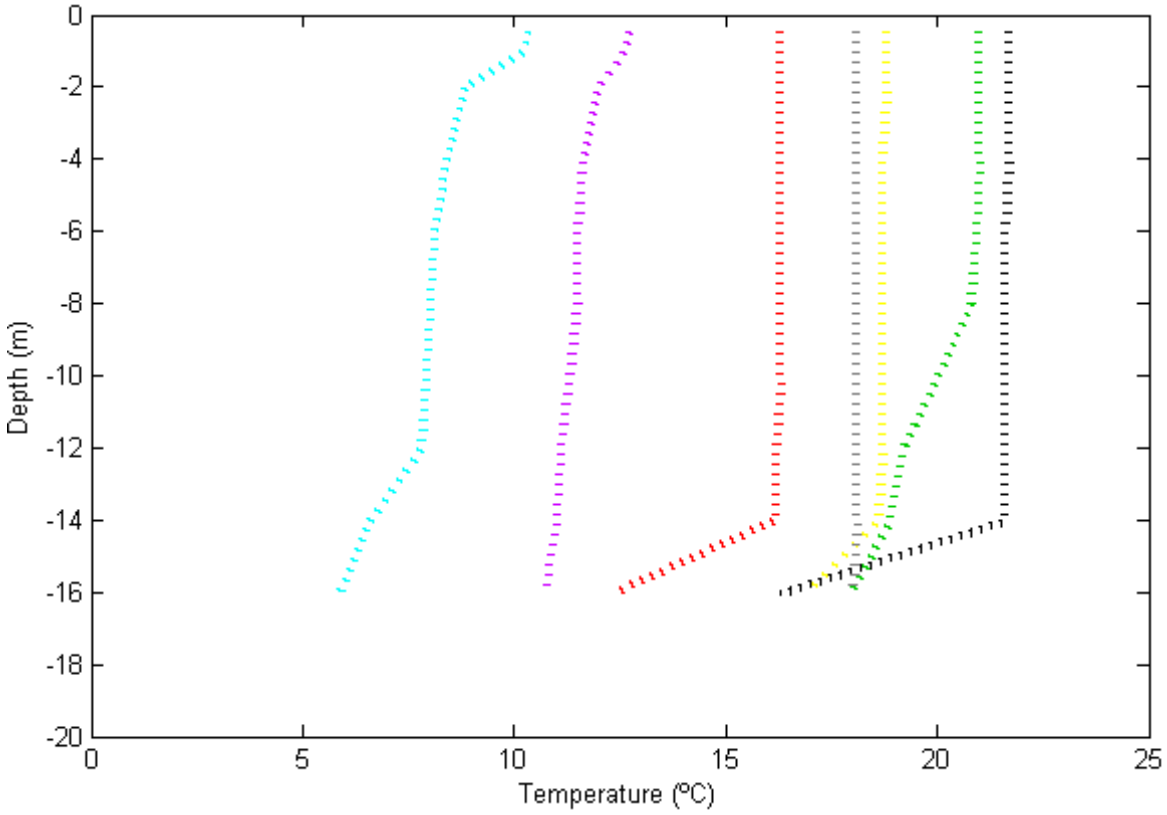


Figure 19: Temperature measurements Lake *Haarlemmermeerse Bos* from 2012. The various lines are different moments of measurement (every four weeks).

7.4 RESULTS OF THE CASE STUDY LAKE *HAARLEMMERMEERSE BOS*

The schematisation of Lake *Haarlemmermeerse Bos* was firstly tested without using a mixing system. In 2013, the bubble plume system in the lake had been turned off, providing data of the lake fully stratified. Figure 20 shows this reference case and the schematisation shows a generally good match with the measurement data.

The used measure for the schematisation's accuracy – also used to calibrate the results – is the root-mean-square error (RMSE) of the temperature, using the same weight for every location in the depth. It is averaged over the several moments of measurements during the year. For the reference case, the RMSE is 2.0 °C.

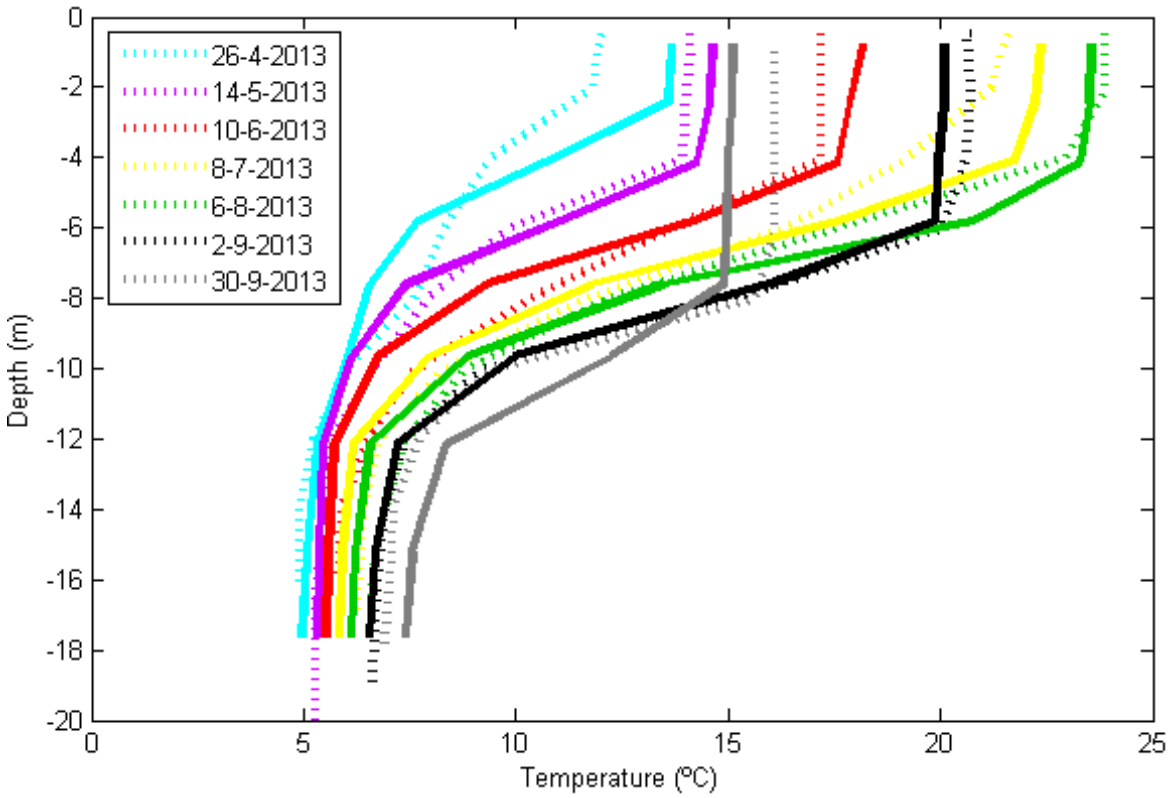


Figure 20: Delft3D output and temperature measurements in Lake *Haarlemmermeerse Bos* (stratified lake, 2013). The various lines are different moment of measurement (every two weeks). Dotted lines are measurements and solid lines are results from the schematisation.

7.4.1 AIRLIFT MIXING

For the scenario with an airlift as mixing system, measurement results from 2012 – the year with mixing – are used. That year, Lake *Haarlemmermeerse Bos* was destratified using four bubble plumes. Figure 21 shows the velocity output in a cross-section of the Delft3D schematisation that uses the airlift. The vertical flows near the airlift and a vertical circulation in the middle are clearly visible.

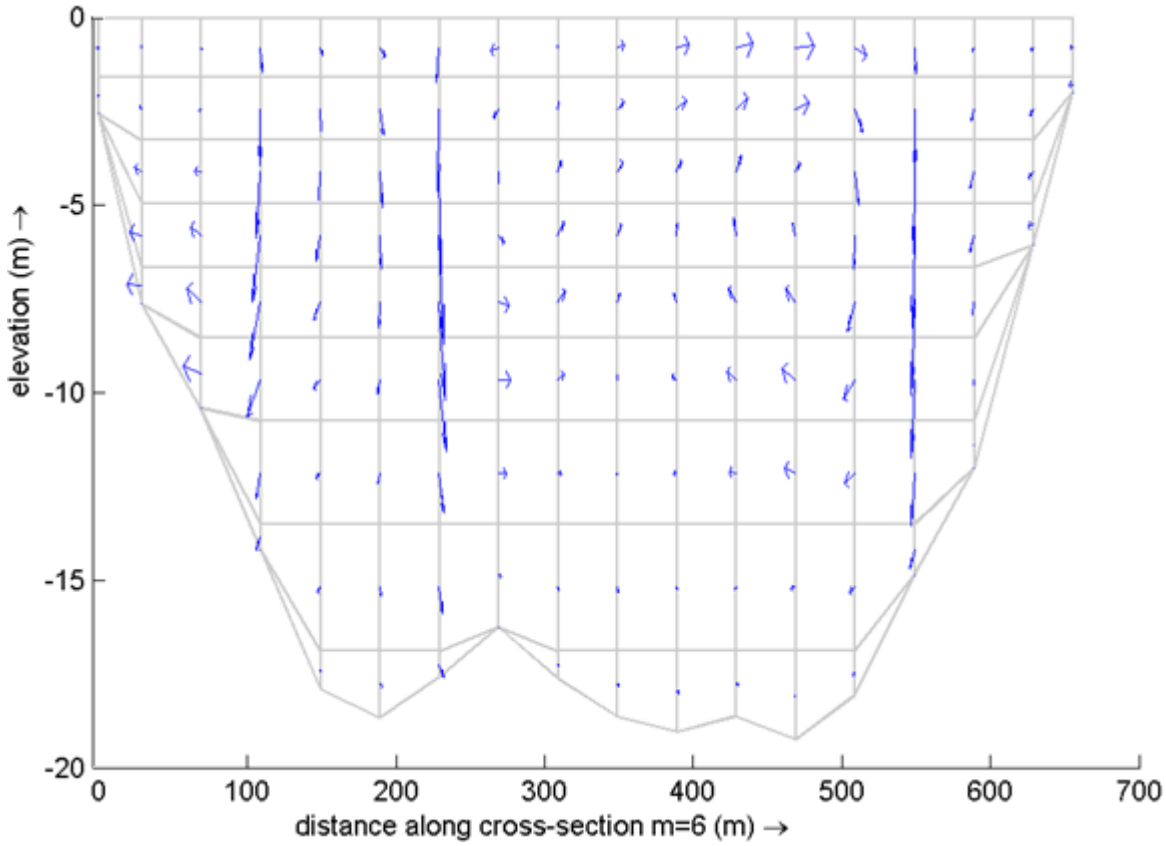


Figure 21: Velocity field in a vertical cross-section of Lake *Haarlemmermeerse Bos* using airlifts as mixing system. The maximum velocity is 8.2 x 10^{-3} m/s. The vertical flows resulting from the three airlifts alongside this cross-section and a vertical circulation in the middle are clearly visible. Note that the depth of the lake is 30x enlarged. Also note that this is a snapshot to show the influence of the airlifts, but results vary in time a lot because of other factors of influence (like wind).

The schematisation's accuracy is a little lower than in the reference case: an RMSE of 2.7 °C, but the overall picture is complete mixing in the vertical, see Figure 22. Two parts of the results are notably different. Firstly, the first temperature profile (the black dotted line) differs significantly from the calculation (solid line); the explanation for this is that probably the mixing system was turned on around 1 April instead of 1 May. (That is done manually without a strictly maintained fixed moment in the year and no log is kept.) The schematisation shows a regular situation that the lake starts developing the thermal stratification in April and that mixing starts from May.

Secondly, there is no mini hypolimnion in the schematisation's result like there is in the measurement data. A recent check on the system by a diving team, however, shows that the aerators at -15 m maximally, while originally intended at -17 m (Gunderson, 2015).

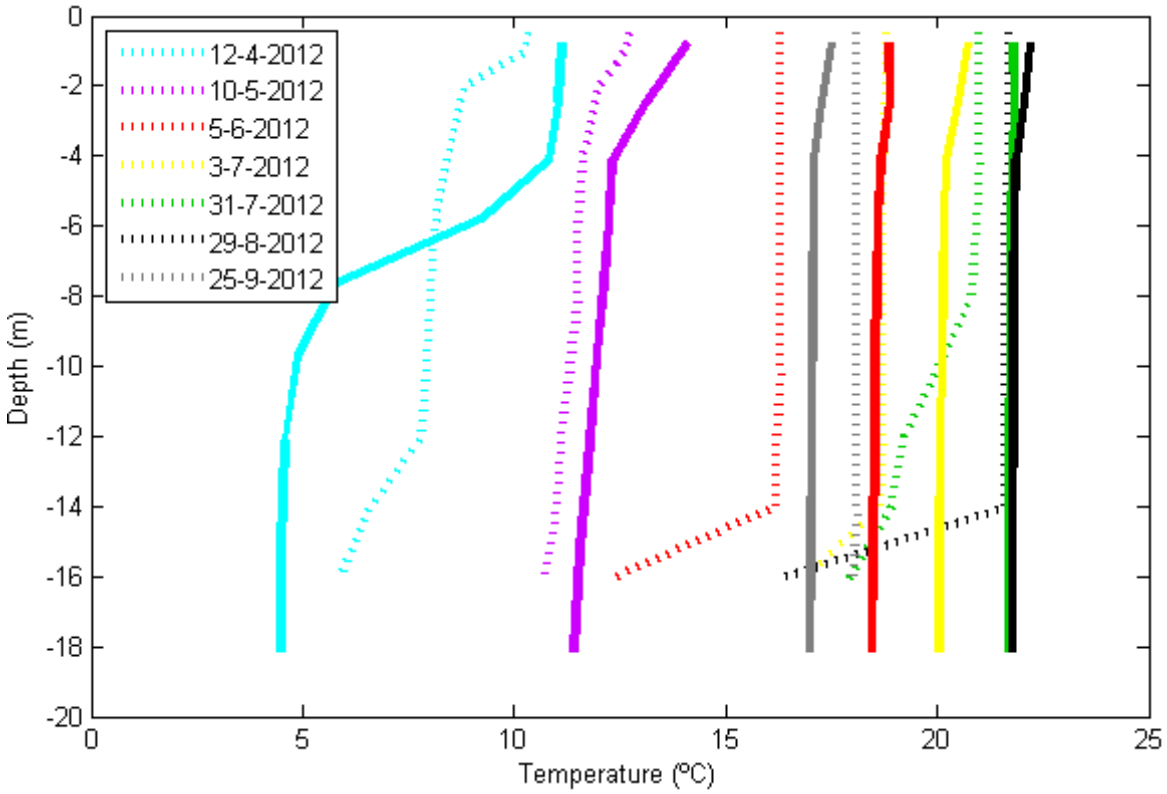


Figure 22: Temperature profiles of mixing with four airlifts and temperature measurements in Lake *Haarlemmermeerse Bos*. The various lines are different moments of measurement (every two weeks). Dotted lines are measurements and solid lines are results from the schematisation.

7.4.2 BUBBLE PLUME MIXING

For the scenario with a bubble plume mixing system, also measurement results from 2012 are used. Figure 23 shows results with a root-mean-square error of 2.6 °C, nearly identical as the airlift results from Figure 22. Even though the RMSE is lower, the bubble plume model seems to be better at handling the minor stratification the measurements show: it mixes the initial stratification slightly slower than the airlift.

A short new run to optimise the amount of air needed to destratify the water provides an interesting new insight. Instead of using the amount of air currently applied in Lake *Haarlemmermeerse Bos*, a significantly lower flow of course reduces the mixing performance of the bubble plume system and a little stratification remains. However, the destratification resulting from airlift does so considerably less.

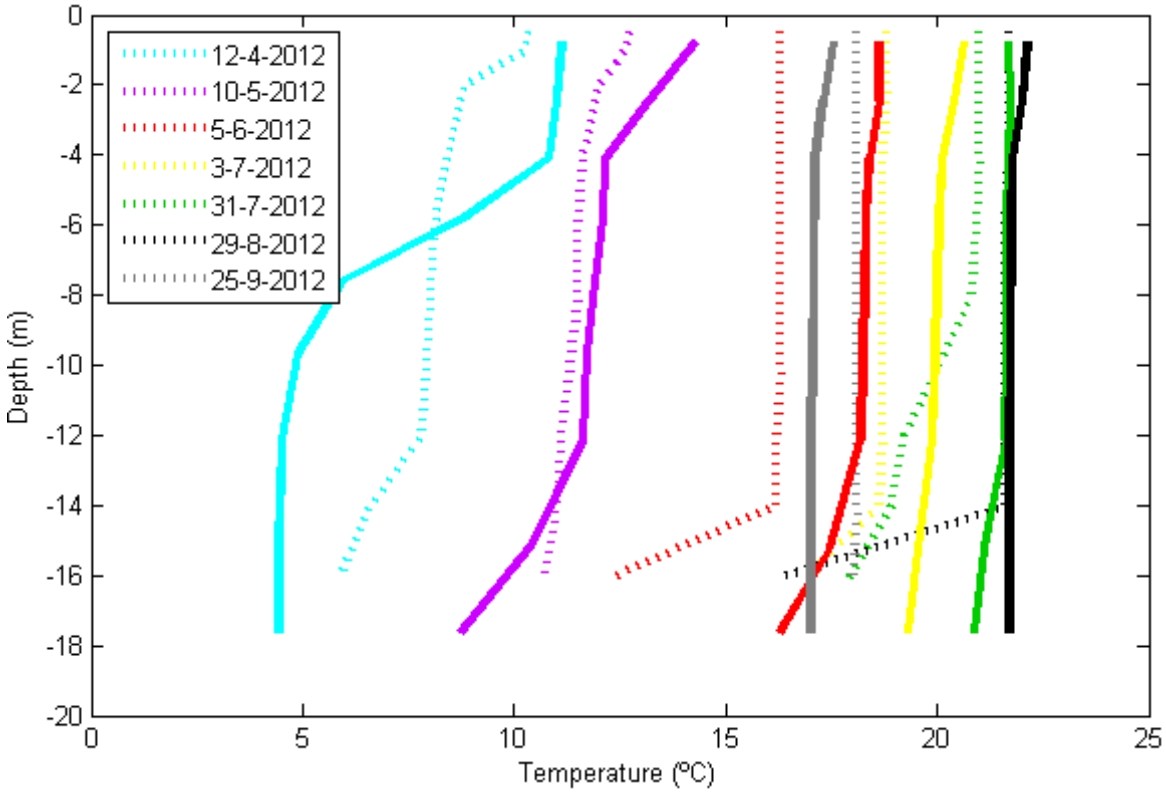


Figure 23: Results Delft3D output and temperature measurements in Lake *Haarlemmermeerse Bos* (lake mixed by bubbles plumes, 2012). The various lines are different moment of measurement (every two weeks). Dotted lines are measurements and solid lines are results from the schematisation.

8 CONCLUSION AND RECOMMENDATIONS

The hypothesis was that an airlift is a more energy efficient structure than a conventional bubble plume system to destratify deep waters.

An artificial mixing system is an important measure for the water board *Rijnland* in order to have healthy waters and a good water quality also for bathing. The mixing is a proven principle to fight the blue algae as it moves blue algae to water where they grow slowly, i.e. dark, turbulent, cold and oxygen-rich waters.

Based on the laboratory experiments and the schematisations, the following observations are made:

- The experiment shows that the airlift destratifies the water volume slightly slower than the bubble plume.
- The schematisation of this experiment shows that the airlift and bubble plume destratify the water volume in almost the same time.
- The schematisation of Lake *Haarlemmermeerse Bos* shows that the airlift destratifies the water a little faster than the bubble plume.

Taking these results into account, the differences between the bubble plume and the airlift are small. Dependent on the particular application of the air mixing system, the balance shifts either in favour of the airlift or in favour of the conventional bubble plume system. Hence, the airlift cannot be confirmed as a generally more energy efficient structure.

However, the schematisation of Lake *Haarlemmermeerse Bos* shows that for a much lower air flow than currently applied, the water is still mostly destratified by the airlift, whereas the bubble plume performs worse. A new research project could investigate the optimal airflow for the airlift to be able to reduce the energy costs and confirm that the airlift is able to remove most of the stratification also with a smaller air flow.

From Lake *Vlietlanden*, it is shown that only removing the thermocline is not necessarily sufficient for reduction of blue algae concentrations. It is recommended to investigate the amount of mixing that is needed for that. Because this higher flow of water can only be induced by line elements instead of point aerators, it may also be interesting to investigate a very wide type of airlift / line element airlift.

Other possibilities to optimise the airlift's performance are to use a trumpet shape bottom end for less inlet energy losses, to change the depth of the top end of the airlift, to change the size and frequency of the bubbles and to determine whether it more efficient to use one bigger structure or several smaller ones.

REFERENCES

Abraham, G., Burgh, P. van der and Vos, P. de (1973). Pneumatic barriers to reduce salt intrusion through locks. Rijkswaterstaat Communications No. 17.

Arcadis (2014). Rapportage Onderzoek KRW maatregelen Nieuwe Meer en Amstelveense Poel.

Asaeda, T. and Imberger, J. (1993). Structure of bubble plumes in linearly stratified environments. *Journal of Fluid Mechanics*, 249, 35-57. http://dx.doi.org/10.1017/S0022112093001065

Buick, R. (2008). When did oxygenic photosynthesis evolve? Philosophical Transactions of the Royal Society of London. B. http://doi.org/10.1098/rstb.2008.0041

Buiter, R. (2013). Belletjes tegen de blauwalg. *Visionair,* 29, 17-19.

Buiter, R., Hoekstra, W.P.M., Lamers, P.P. (2013). *De groene belofte: Algen*. Zutphen: Stichting Biowetenschappen en Maatschappij.

Burchard, H. and Baumert, H. (1995). On the performance of a mixed-large model based on the k-epsilon turbulence closure. *Journal of Geophysical Research*, 100 (C5): 8523–8540.

Calvin, M. (1961). The Path of Carbon in Photosynthesis. www.osti.gov/cgi-bin/rd_accomplishments/display_biblio.cgi?id=ACC0327&numPages=49&fp=N

Carmichael, W.W. (1992). Cyanobacteria secondary metabolites — the cyanotoxins. *Journal of applied bacteriology,* 72, 445-459. http://dx.doi.org/10.1111/j.1365-2672.1992.tb01858.x

Castenholz, R. W., and Waterbury, J. B. (1989). Group I. Cyanobacteria. *Bergey's Manual of Systematic Bacteriology*, vol. 3, pp. 1710–1728. Edited by N. R. Krieg & J. G. Holt. Baltimore: Williams & Wilkins.

Chorus, I. (2012). Current approach to Cyanotoxin risk assessment, risk management and regulations in different countries. *Federal Environment Agency, Germany.*

Codd, G. A. and Bell, S. G. (1996). *The occurrence and fate of blue-green algal toxins in freshwaters*. HMSO, London.

Codd, G.A., Morrison, L.F. and Metcalf, J.S. (2005). Cyanobacterial toxins: Risk management for health protection. *Toxicol. Appl. Pharmacol,* 203, 264–272.

De Toren (2014). ChristenUnie heeft vragen over blauwalg. http://detoren.net/artikelen/Nieuws/Christen_Unie_heeft_vragen_over_blauwalg_84488/8/1. Viewed on 29 Oct 2015.

Deltares (2011a). Delft3D-FLOW User Manual. Chapter B.22 Bubble screen.

Deltares (2011b). Hydrodynamic simulations of the reduction of Microcystis blooms by bubble plumes in deep lakes.

Deltares (date unknown). Delft3D 4 Suite (structured). https://www.deltares.nl/en/software/delft3d-4-suite/. Viewed on 18 Nov 2015.

Dittmann, E. and Wiegand, C. (2006). Cyanobacterial toxins—Occurrence, biosynthesis and impact on human affairs. *Molecular Nutrition Food Research,* 50, 7–17.

EU Bathing Water Directive (2006). Downloaded from http://eur-lex.europa.eu/legal-content/EN/TXT/?uri=CELEX:32006L0007. Viewed on 2 Nov 2015.

EU Water Framework Directive (2000). Downloaded from http://eur-lex.europa.eu/legal-content/EN/TXT/?uri=CELEX:32000L0060. Viewed on 2 Nov 2015.

European Environment Agency (2014). State of bathing waters. http://www.eea.europa.eu/themes/water/interactive/bathing/state-of-bathing-waters. Viewed on 3 Nov 2015.

Fannelop, T. K. and Sjoen, K. (1980). *Hydrodynamics of underwater blowouts*. Ship Research Institute of Norway, Marine Technology Centre, Trondheim.

Fawell, J.K., Hart, J., James, H.A. and Parr, W. (1993). Blue-green algae and their toxins — analysis, toxicity, treatment and environmental control. *Water supply*, 11, 109-121.

FishFlow Innovations (2011). Airlift placed in Ursemmerplas. http://fishflowinnovations.nl/en/news/news/airlift-placed-in-ursemmerplas. Viewed on 27 Oct 2015.

FishFlow Innovations (2013). Airlift placed in Kotermeerstal. http://fishflowinnovations.nl/en/news/news/airlift-placed-in-kotermeerstal. Viewed on 27 Oct 2015.

FishFlow Innovations (date unknown). Airlift. http://fishflowinnovations.nl/en/our-innovations/airlift. Viewed on 27 Oct 2015.

Garcia-Pichel, F., Belnap, J., Neuer, S., and Schanz, F. (2003). Estimates of global cyanobacterial biomass and its distribution. *Algological Studies*, v. 109, p. 213-227. http://dx.doi.org/10.1127/1864-1318/2003/0109-0213

Gons, H.J. (1977). On the light-limited growth of Scenedesmus protuberans Fritsch. Thesis, University of Amsterdam.

Gunderson, A. (2015). Situatie pontons februari 2015. https://www.youtube.com/watch?v=8CTn7v1Iekw. Viewed on 1 Jun 2015.

Hoogheemraadschap van Rijnland (2000). Beleid diepe putten. http://decentrale.regelgeving.overheid.nl/cvdr/xhtmloutput/Historie/Hoogheemraadschap%20van%20Rijnland/272319/272319_1.html. Viewed on 4 Nov 2015.

Hoogheemraadschap van Rijnland (2014). Nota Schoon Water 2. http://www.rijnland.net/plannen/downloads-plannen/nota-schoon-water-2.pdf

Hoogheemraadschap van Rijnland (2015). Rijnland in vogelvlucht. https://www.rijnland.net/over-rijnland/kijkje-in-de-keuken/rijnland-in-vogelvlucht. Viewed on 4 Nov 2015.

Hoogheemraadschap van Rijnland (date unknown-a). 1255: De heemraden van Spaarndam. https://www.rijnland.net/over-rijnland/erfgoed/artikelen-geschiedenis-en-canon/1255-de-heemraden-van-spaarndam. Viewed on 13 Oct 2015.

Hoogheemraadschap van Rijnland (date unknown-b). Interactive map viewer Rijnland. http://rijnland.webgispublisher.nl/?map=Rijnland_viewer. Viewed on 11 Nov 2015.

Hoogheemraadschap van Rijnland (date unknown-c). Wat doet Rijnland. https://www.rijnland.net/over-rijnland/taken. Viewed on 13 Oct 2015.

Huisman, J. and Hulot, F. (2005). Population Dynamics of Harmful Cyanobacteria. In J. Huisman, H. P. Matthijs & P. Visser (Eds.), *Harmful Cyanobacteria,* 3, 143-176.

Huisman, J., Sharpies, J., Stroom, J.M., Visser, P.M., Kardinaal, W.E.A., Verspagen, J.M.H., Sommeijer, S B. (2004). Changes in turbulent mixing shift competition for light between phytoplankton species. *Ecology,* 85, 2960-2970.

Ibelings, B. W., Kroon, B. M. A. and Mur, L. R. (1994). Acclimation of photosystem II in a cyanobacterium and a eukaryotic green alga to high and fluctuating photosynthetic photon flux densities, simulating light regimes induced by mixing in lakes. *New Phytologist*, 128, 407–424. http://dx.doi.org/10.1111/j.1469-8137.1994.tb02987.x

Ibelings, B.W., Mur, L.R. and Walsby, A.E. (1991). Diurnal changes in buoyancy and vertical distribution of Microcystis in two shallow lakes. *Journal of Plankton Research*, 13, 419–436.

Interprovinciaal Overleg, Unie van Waterschappen and Rijkswaterstaat (2015). Zwemwater. http://www.zwemwater.nl/. Viewed on 16 Oct 2015.

Invoeringswet Waterwet (2015). Downloaded from http://wetten.overheid.nl/BWBR0026710/geldigheidsdatum_13-10-2015/informatie. Viewed on 13 Oct 2015.

Jungo, E., Visser, P.M., Stroom, J. and Mur, L. (1993). Artificial mixing to reduce growth of the blue green alga Microsystis in Lake Nieuwe Meer, Amsterdam: an evaluation of 7 years of experience.

Kobus, H.E. (1975). On the use of air-bubble screens as oil barriers. *International Association for Hydraulic Research*, 356-363.

Konopka, A. E. (2014). Cyanobacteria. *AccessScience*. McGraw-Hill Education. http://dx.doi.org/10.1036/1097-8542.174950

Lalli, C. M. and Parsons, T.T. (1997). *Biological Oceanography: An Introduction (Second Edition)*. Oxford: Elsevier. http://dx.doi.org/10.1016/B978-0-7506-3384-0.50085-2

Lehrer, I. (1980). A theoretical criterion of transition in the free motion of single bubbles and drops. *AIChE Journal*, 26, 170-172.

Liere, L. van, Mur, L.R., Gibson, C.E. and Herdman, M. (1979). Growth and physiology of Oscillatoria agardhii and some related species, a survey. *Dev. Hydrobiol.*, 2, 67-77.

Lurling, M. and Faassen, E. (2013). Dog poisoning associated with a Microcystis aeruginosa bloom in the Netherlands. *Toxins*, 5, 556-567.

Mayer, D. (2008). File:Simple photosynthesis overview.svg. Downloaded from https://en.wikipedia.org/wiki/File:Simple_photosynthesis_overview.svg. Viewed on 25 Nov 2015.

Mcdougall, T.J. (1978). Bubble plumes in stratified environments. *Journal of Fluid Mechanics,* 85, 655-672. http://dx.doi.org/10.1017/S002211207800084

Medrano, E. A. (2014). Physical aspects explaining cyanobacteria scum formation in natural systems (PhD thesis).

Michielsen, B. (2002). De Waterkwaliteit van Rijnlands Diepe Putten. Report from Hoogheemraadschap van Rijnland.

Michielsen, B. and Ibelings, B. (2002). Rijnlands diepe putten: drijflagen van cyanobacteriën, ondanks goede waterkwaliteit?. *H twee O*, 35, 17.

Milgram, J.H. (1983). Mean flow in round bubble plumes. *Journal of Fluid Mechanics*, 133, 345-376. http://dx.doi.org/10.1017/S0022112083001950

Molenaar, E. (date unknown). Downloaded from: Noordhollands Dagblad (2013). Export succesvolle buis tegen blauwalg. http://www.noordhollandsdagblad.nl/stadstreek/enkhuizen-westfriesland/article23820293.ece. Viewed on 7 Nov 2015.

Moore, D.W. (1959). The rise of a gas bubble in a viscous liquid. *Journal of Fluid Mechanics*, 6, 113-130. http://dx.doi.org/10.1017/S0022112059000520

Mur, L.R., Skulberg, O.M. and Utkilen, H. (1990). Cyanobacteria in the environment, in Chorus, I., and Bartram, J. [Eds], *Toxic Cyanobacteria in Water: A guide to their public health consequences, monitoring and management*. ISBN 0-419-23930-8.

Nationaal Wateroverleg (2012). Blauwalgenprotocol 2012.

Niel, C.B. van (1931). On the morphology and physiology of the purple and green sulfur bacteria.

Oosterbaan, J. and Heuzen, M. (2011). Artificial mixing in Rijnland; facts and figures. Presentation for ONEP.

Paerl, H.W. and Ustach, J.F. (1982). Blue-green algal scums: An explanation for their occurrence during freshwater blooms. *Limnology and Oceanography*, 27, 212-217.

Paerl, H.W., Tucker, J. and Bland, P.T. (1983). Carotenoid enhancement and its role in maintaining blue-green (Microcystis aeruginosa) surface blooms. *Oceanography,* 28, 847-857.

Pierce, J., and Omata, T. (1988). Uptake and utilization of inorganic carbon by cyanobacteria. *Photosynthesis Research*, (1988)16:141-154.

Pietrzak, J. (2012). Stratified Flows. TU Delft CIE 5302 Draft lecture notes.

Reynolds, C.S. (1987). Cyanobacterial water blooms. *Advances in Botanical Research*, 13, 67-143.

Reynolds, C.S. (2007). Variability in the provision and function of mucilage in phytoplankton: facultative responses to the environment. *Hydrobiologia*, 578, 37-45.

Reynolds, O. (1895). On the Dynamical Theory of Incompressible Viscous Fluids and the Determination of the Criterion. Philosophical Transactions of the Royal Society of London. A, 186, 123–164. Retrieved from http://www.jstor.org/stable/90643

Rodi, W. (1984). Turbulence models and their application in hydraulics: a state of the art review. Delft : International association for hydraulic research.

RTV NH (2014). Weer zwemverbod voor Ursemmerplas. http://www.rtvnh.nl/nieuws/145076/weer-zwemverbod-voor-ursemmerplas. Viewed on 27 Oct 2015.

RTV NH (2015). Zwemverbod Ursemmerplas na aantreffen hoge concentratie blauwalg. http://www.rtvnh.nl/nieuws/168809/zwemverbod-ursemmerplas-na-aantreffen-hoge-concentratie-blauwalg. Viewed on 27 Oct 2015.

Scheffer, M. (1998). *Ecology of shallow lakes*. Springer US.

Schopf, J. W. (2012). The fossil record of cyanobacteria. In B. A. Whitton (Ed.), *Ecology of Cyanobacteria II: Their Diversity in Space and Time* (pp. 15–36). Springer Netherlands. http://dx.doi.org/ 10.1007/978-94-007-3855-3

Shapiro, J. (1997). The role of carbon dioxide in the initiation and maintenance of blue-greens dominance in lakes. *Freshwater Biology*, 37, 307-323.

Silva, P. C. and Moe, R. L. (2014). Cyanophyceae. *AccessScience*. McGraw-Hill Education. http://dx.doi.org/10.1036/1097-8542.175300

Sirenko, L.A. (1972). *Physiological base of multiplication of blue-green algae in reservoirs*. Kiev: Naukova Dumka. (in Russian; translation of pages 88-162 supplied by The British Library The world's knowledge).

Sirenko, L.A., Stetsenko, N.M., Arendarchuk, VV. and Kuz'menko, M.K. (1968). Role of oxygen conditions in the vital activity of certain blue-green algae. *Microbiology*, 37, 199-202.

Skulberg, O.M., Carmichael, W.W., Codd, G.A. and Skulberg, R. (1993). Taxonomy of toxic Cyanophyceae (Cyanobacteria). In: I. R. Falconer [Ed.] *Algal Toxins in Seafood and Drinking Water*. Academic Press Ltd., London, 145-164.

Stone, D. and Bress, W. (2007). Addressing public health risks for cyanobacteria in recreational freshwaters: The Oregon and Vermont framework. *Integr Environ Assess Manag*, 3: 137–143. http://dx.doi.org/ 10.1002/ieam.5630030112

STOWA (1993). Ecologische beoordeling en beheer van oppervlaktewater. http://krw.stowa.nl/Projecten/EBEO___ecologische_beoordelingssystemen.aspx. Viewed on 4 Nov 2015.

STOWA (date unknown). Cyanobacteriën. http://cyanobacterien.stowa.nl/Zwemwater/Beating_the_blues.aspx?pId=245. Viewed on 12 Nov 2015.

Stroom, J.M. and Schaik, F. van (2007). Beknopte evaluatie mengsystemen Bosplas en Nieuwe Meer. Hoogheemraadschap van Rijnland, Leiden.

Van Liere, L., and Walsby, A. E. (1982). Interactions of cyanobacteria with light. In N.G. Carr and B.A. Whitton [Eds], *The Biology of the Cyanobacteria*. Oxford: Blackwell Science Publications, 9(45).

Verspagen, J. M. H., Passarge, J., J¨ohnk, K. D., Visser, P.M., Peperzak, L., Boers, P., Laanbroek, H. J., & Huisman, J. (2006). Water management strategies against toxic Microcystis blooms in the Dutch delta. *Ecological Applications*, 16, 313-327.

Visser, P. M., Ibelings B. W., Mur L. R., and Walsby A. E. (2005). The ecophysiology of the harmful cyanobacterium Microcystis: features explaining its success and measures for its control, p. 109–142. In J. Huisman, H.C.P. Matthijs, and P.M. Visser (ed.). *Harmful cyanobacteria*. Springer, Dordrecht, The Netherlands.

Walsby, A.E. (1987). Mechanisms of buoyancy regulation by planktonic cyanobacteria with gas vesicles. In: P. Fay and C. Van Baalen [Eds]. *The Cyanobacteria*. Elsevier, Amsterdam, 377-414.

Walsby, A.E. and Bleything, A. (1988). The dimensions of cyanobacterial gas vesicles in relation to their efficiency in providing buoyancy and withstanding pressure. *Journal of General Microbiology*, 134, 2635-2645.

Water on the Web (2015). Density Stratification. http://www.waterontheweb.org/under/lakeecology/05_stratification.html. Viewed 25 Nov 2015.

Waternet (2013a). Beating the Blues. http://www.innovatie.waternet.nl/projecten/beating-the-blues-blauwalgbestrijding-in-nederland/. Viewed on 12 Nov 2015.

Waternet (2013b). Fact sheet vertical mixing, Beating the Blues. http://cyanobacterien.stowa.nl/upload/Cyanobacteri%C3%ABn/Zwemwatercontrole/cura-mengen-verticaal.pdf. Viewed on 25 Nov 2015.

Waterwet (2015). Downloaded from http://wetten.overheid.nl/BWBR0025458/geldigheidsdatum_13-10-2015/informatie. Viewed on 13 Oct 2015.

Wesselingh, J.A. (1987). The velocity of particles, drops and bubbles. *Chem. Eng. Process.*, 21, 9-14.

Wet Verontreiniging Oppervlaktewateren (2015). Downloaded from http://wetten.overheid.nl/BWBR0002682/geldigheidsdatum_13-10-2015/informatie. Viewed on 13 Oct 2015.

World Health Organization (2003). Cyanobacterial toxins: Microcystin-LR in Drinking-water. Background document for development of WHO Guidelines for Drinking-water Quality, 1998.

Yoo, R. S. (1995). *Cyanobacterial (blue-green algal) toxins: A resource guide*, Denver, CO: Published by the AWWA Research Foundation and American Water Works Association.

Zohary, T. and Breen, C.M. (1989). Environmental factors favoring the formation of Microcystis aeruginosa hyperscums in a hypertrophic lake. *Hydrobiologia*, 178, 179-192.

APPENDIX A: MATLAB SCRIPTS FOR EXPERIMENT

XML-conversion

```
% loadUltimaXML (v4.1)
% 29/05/2012
%
% Author: Koen Hilgersom (2012)
%
% This script loads part of the data from the Ultima produced XML-files and
% puts it into arrays called Data (distance, Stokes, anti-Stokes, and fiber-
% optic temperature data), time (time vector), and PT100 (reference
% temperature data). The data is loaded for the channels specified. The
% arrays are saved in the folder specified.
%
%------------------------------------------------------------------------
%     Copyright (C) 2012 TechnischeUniversiteit Delft,
%         Koen Hilgersom
%         K.P.Hilgersom@tudelft.nl (correspondence)
%
%------------------------------------------------------------------------


clear
mainDir='≪data location≫'; %main directory (excluding the names of the channel folders)
channels=[1]; %select the desired channels: [1,2,3,4]

for z=channels
files=dir([mainDirfilesep 'channel ' num2str(z) filesep '*.xml']);

   PT100=NaN(length(files),2);
time=NaN(length(files),1);
   Data=NaN(length(files),1,4);

tic
for k=1:length(files)
XRead=xmlread([mainDirfilesep 'channel ' num2str(z) filesep files(k).name]);
child                                                                                                    =
XRead.getChildNodes.item(0).item(1).item(XRead.getChildNodes.item(0).item(1).getLength-2);
childNodes = child.getChildNodes;
numChildNodes = childNodes.getLength/2;
if size(Data,2)<numChildNodes
         Data=cat(2,Data,NaN(length(files),numChildNodes-size(Data,2),4));
end
for n=1:numChildNodes
Data(k,n,:)=str2num(char(child.item(2*(n-1)).item(0).getData));
end
      A=char(XRead.item(0).item(1).item(7).item(0).getData);
      time(k)=datenum(str2num([A(1:4) ',' A(6:7) ',' A(9:10) ',' A(12:13) ',' A(15:16) ',' A(18:19)]));
```

```
PT100(k,:)=[str2num(XRead.item(0).item(1).item(11).item(5).item(0).getData),str2num(XRead.i
tem(0).item(1).item(11).item(7).item(0).getData)];
end
toc

save([mainDirfilesep 'channel ' num2str(z) '.mat'],'Data','time','PT100')
end
```

Time correction

```
clc
clear
format long

mainDir='≪data location≫';
timeCorr=1/24; %time correction (days) (e.g., when -22/24, 22 hours are subtracted from the
time saved by the machine)
channels=[1];

for k=channels
load([mainDirfilesep 'channel ' num2str(k) ]);
time = time + timeCorr;
   [Temp,Sto,ASto,time,Dist,PT100]=prepData(Data,time,PT100);
   save([mainDirfilesep 'channel ' num2str(k) 'pf'],'Dist','Temp','Sto','ASto','time','PT100');
%    save([mainDirfilesep 'channel ' num2str(k) 'p'],'Dist','Temp','time','PT100');
end
```

Plot data

```
%% Script instructions

% Fill in data location, relevant start and stop time
% Choose filter settings
% Choose whether to display absolute or relative temperatures
% Choose plot ranges. Wider plot ranges than data ranges give white
% borders.
% Choose plot type.

clc, clear, format long, close all
plottype = 'contour';      %'imagesc' or 'contour'
prestype = 'diff';         %'mean', 'start' or 'diff'
saveDir = ['≪save location≫' plottype];

%% 1. data information
%data location
labresults = {
≪data locations≫
   };

%relevant time range
TimeMin = {
```

```
   '≪dd/mm/yyyy HH:MM:SS≫', ...
   };
TimeMax = {
   '≪dd/mm/yyyy HH:MM:SS≫', ...
   };

%relevant spatial range
Xmin = 138;
Xmax = 242;

%% data plots
for ii = 1:max(size(labresults))

%% read data
mainDir = labresults{ii};
k = 1;                  %select the desired channels: [1,2,3,4]
load( [mainDirfilesep 'channel ' num2str(k) 'pf'] );

RanT = find(time >datenum(TimeMin{ii},'dd/mm/yyyy HH:MM:SS') & time
<datenum(TimeMax{ii},'dd/mm/yyyyHH:MM:ss'));
RanX = Dist>Xmin&Dist<Xmax;
RanTemp = Temp(RanT,RanX).';
RanTemp_Size = size(RanTemp);

%% noise filter
RanFilterTime = 7;        %filter range in time
RanFilterSpace = 7;       %filter range in space
RanTemp2 = medfilt2(RanTemp,[RanFilterTimeRanFilterSpace]);

%% presenting temperatures
switchprestype
case 'mean'          %proportional to the mean, base value = 0
      RanTemp2_Mean_AfterFilter = nanmean(nanmean(RanTemp2));
      RanTemp3 = (RanTemp2 - RanTemp2_Mean_AfterFilter) / RanTemp2_Mean_AfterFilter;
case 'start'         %proportional to the startvalue, base value = 0
      Temp_t0          =          nanmean(min(round(RanTemp(ceil(RanTemp_Size(1)*0.3):end-
1,3:14)*100)/100));
      RanTemp3 = (RanTemp2 - Temp_t0) / Temp_t0;
case 'diff'          %absolute difference, start temperature = 0
      Temp_t0          =          nanmean(min(round(RanTemp(ceil(RanTemp_Size(1)*0.3):end-
1,3:14)*100)/100));
      RanTemp3 = RanTemp2 - Temp_t0;
otherwise
      RanTemp3 = RanTemp2;
end

%% plot ranges
%temperature range
TempLow   = 0;
TempRes   = 0.6;
TempHigh  = 5;
```

```
switchprestype
case 'mean'
TempLow   = -0.25;
TempRes   = 0.25;
TempHigh  = 1.75;
case 'start'
TempLow   = 0;
TempRes   = 0.05;
TempHigh  = 0.4;
case 'diff'
TempLow   = 0;
TempRes   = 0.8;
TempHigh  = 6.4;
end

%time range
TimeStart = 0;
TimeRes   = 1;
TimeStop  = 10;

%depth range
DepthStart = 0;
DepthRes   = 0.25;
DepthStop  = 1.45;

%% make plots
plotname = mainDir(78:end);
ScrSize = get(groot,'ScreenSize');
figure('Name',plotname,'NumberTitle','off','Visible','on','Position',[1 1 ScrSize(3)/2 ScrSize(4)]);
%Position[left bottom width height]
clf

switchplottype
case 'imagesc'
colormap(jet(256))
Trange = [TempLowTempHigh];
DepthAxis = [0 ((Xmax-Xmin)/70)]; %data to plot
TimeAxis = [0 (datenum(TimeMax{ii})-datenum(TimeMin{ii}))*60*24]; %data to plot
imagesc(TimeAxis,DepthAxis,RanTemp3,Trange)
      %hold on
set(gca,'YLim',[DepthStartDepthStop]);
set(gca,'YTick',DepthStart : DepthRes : DepthStop);
set(gca,'XLim',[TimeStartTimeStop]);
set(gca,'XTick',TimeStart : TimeRes : TimeStop);
      %datetick('y','HH:MM','keeplimits','keepticks');
title(plotname,'Interpreter','none')
xlabel('time (minutes)');
ylabel('depth (metres)');
colorbar
case 'contour'
Trange = TempLow :TempRes : TempHigh;
```

```
DepthAxis = 0 :(Xmax-Xmin)/70 / (RanTemp_Size(1)-1):(Xmax-Xmin)/70; %data to plot; length DepthAxis = length Rantemp2
TimeAxis = 0 :(datenum(TimeMax{ii})-datenum(TimeMin{ii}))*60*24 / (RanTemp_Size(2)-1):(datenum(TimeMax{ii})-datenum(TimeMin{ii}))*60*24; %data to plot; length TimeAxis = length Rantemp2
contour(TimeAxis,DepthAxis,RanTemp3,Trange,'ShowText','on','LineColor','k')
set(gca,'YLim',[DepthStartDepthStop]);
set(gca,'YTick',DepthStart : DepthRes : DepthStop);
set(gca,'YDir','reverse');
set(gca,'XLim',[TimeStartTimeStop]);
set(gca,'XTick',TimeStart : TimeRes : TimeStop);
    %datetick('x','HH:MM','keeplimits','keepticks');
title(plotname,'Interpreter','none')
xlabel('time (minutes)');
ylabel('depth (metres)');
end

savename = [mainDir(60:end) '_' plottype '_' prestype];
savefig([saveDirsavename]);
saveas(gcf,[saveDirsavename '.png'])

end
```

APPENDIX B: RESULTS LAB EXPERIMENT

This appendix contains the measurements results from the laboratory experiments with the single bubble plume (figure B1) and the airlift (figure B2). Table B1 summarises these results.

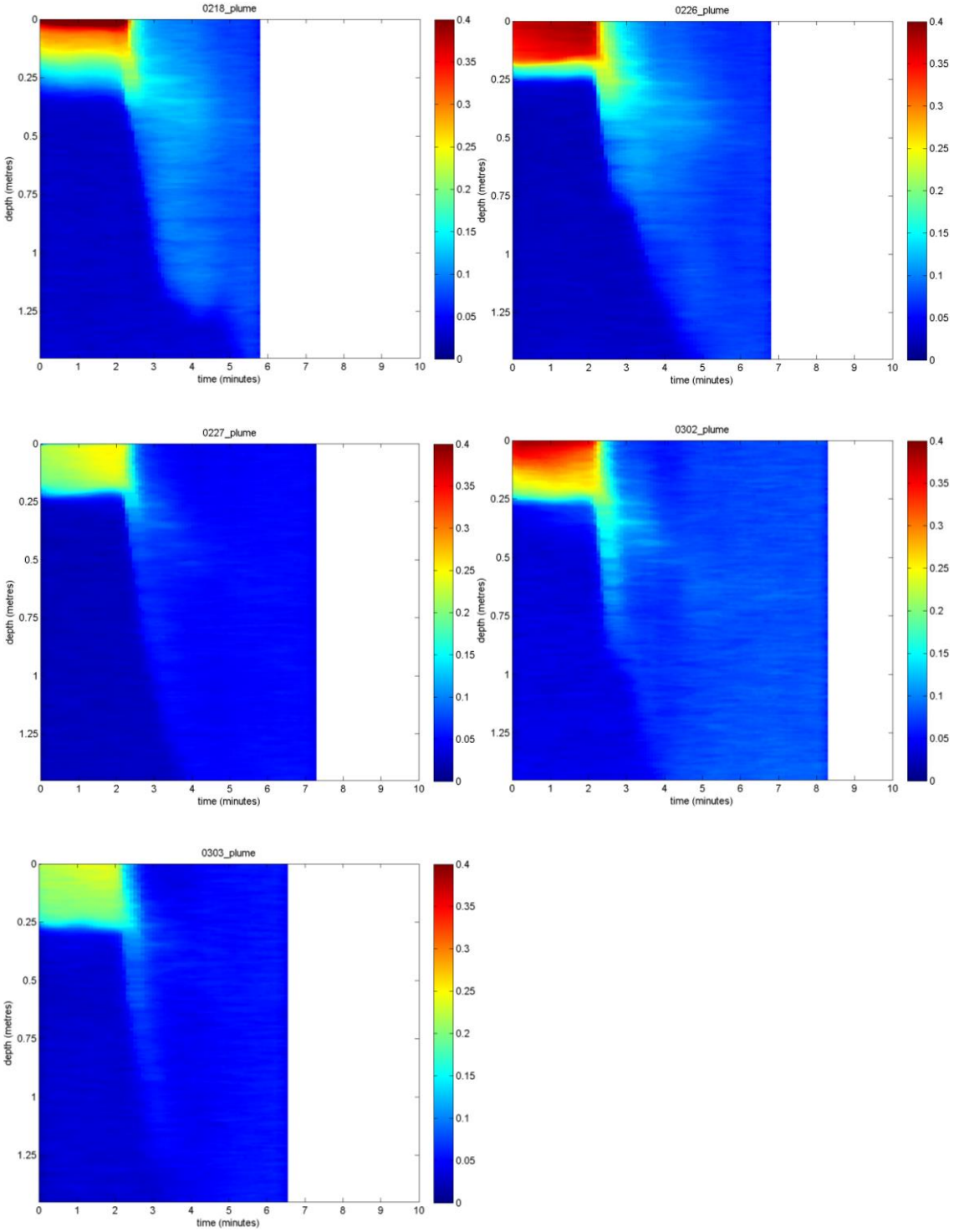
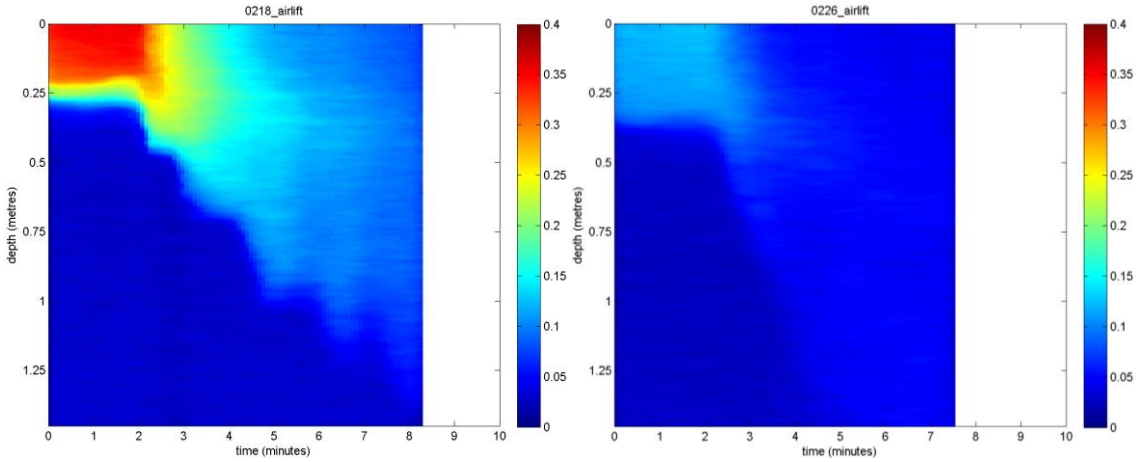
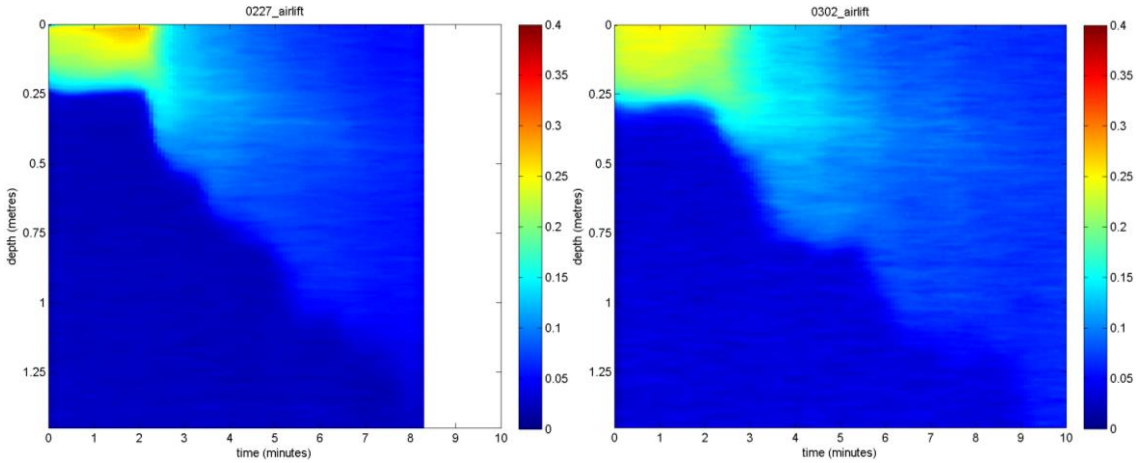


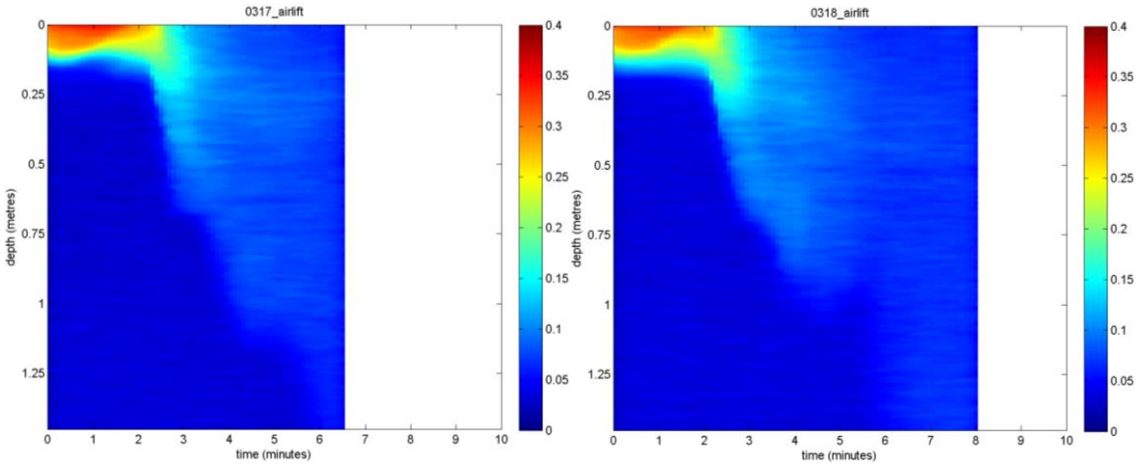
Figure B1: Temperature in space and time during the laboratory experiment with the bubble plume; five repetitions. The temperature is presented as a ratio of the hypolimnion starting temperature added to the hypolimnion starting temperature. 0.4 means that the temperature is 40% higher than the hypolimnion in the beginning.


0218_airlift
depth (metres)
time (minutes)

0226_airlift
depth (metres)
time (minutes)


0227_airlift
depth (metres)
time (minutes)

0302_airlift
depth (metres)
time (minutes)


0317_airlift
depth (metres)
time (minutes)

0318_airlift
depth (metres)
time (minutes)

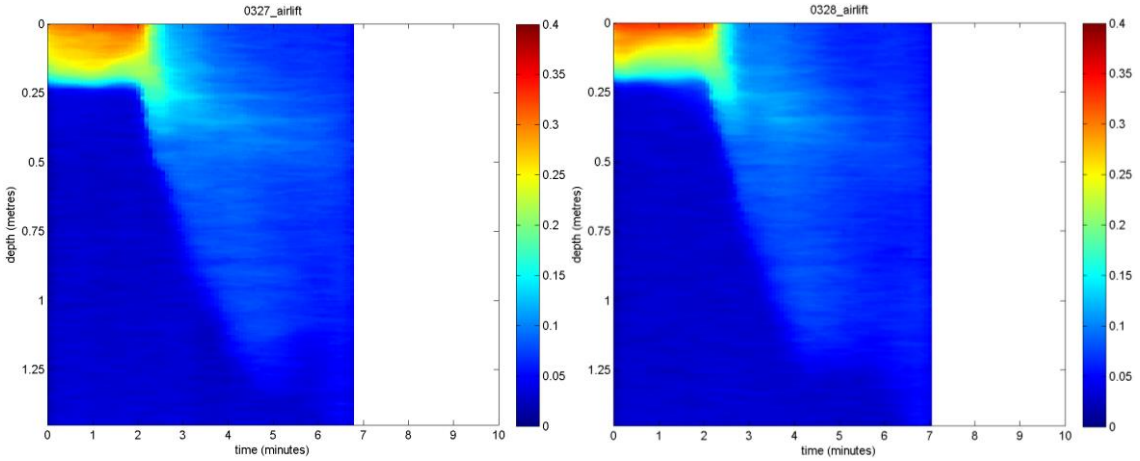


Figure B2: Temperature in space and time during the laboratory experiment with the airlift; eight repetitions. The temperature is presented as a ratio of the hypolimnion starting temperature added to the hypolimnion starting temperature. 0.4 means that the temperature is 40% higher than the hypolimnion in the beginning. Airlift #5-8 were a test for an optimisation by lowering the tube 10 cm and are a little bit faster.

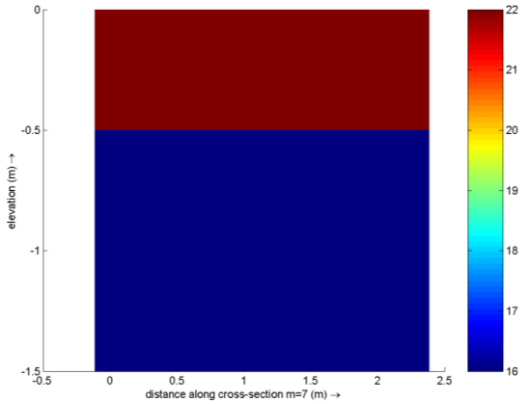
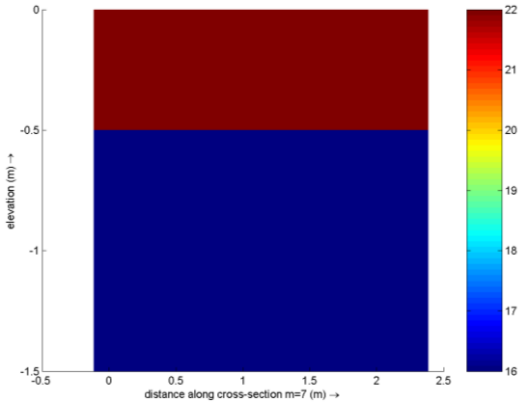
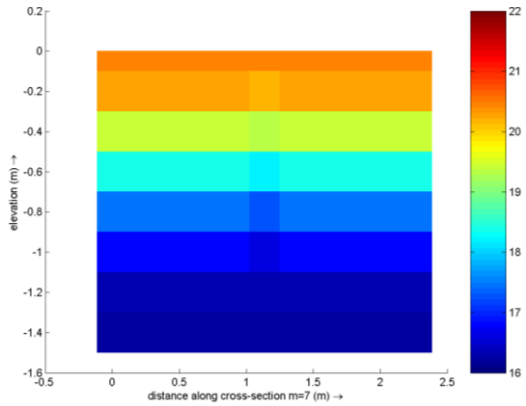
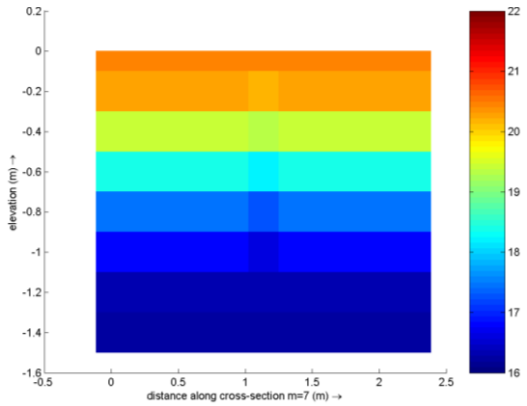
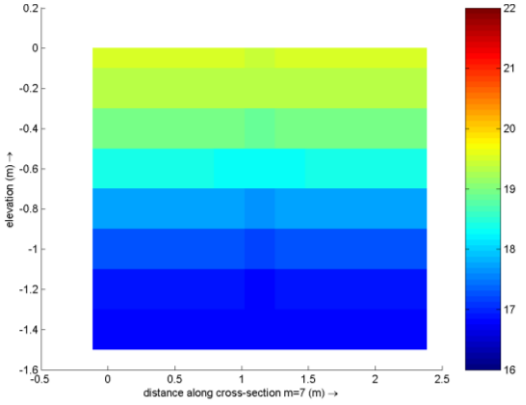
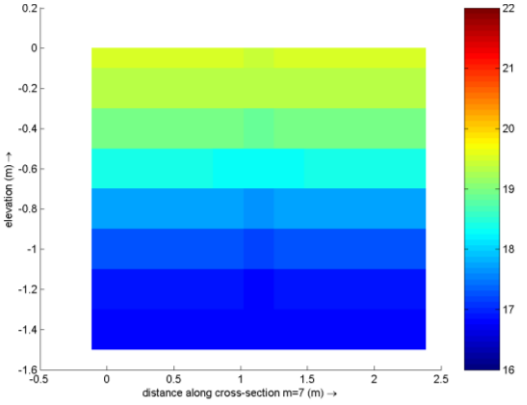
#1	Plume	5.8
#2	Plume	6.8
#3	Plume	7.2
#4	Plume	8.2
#5	Plume	6.5

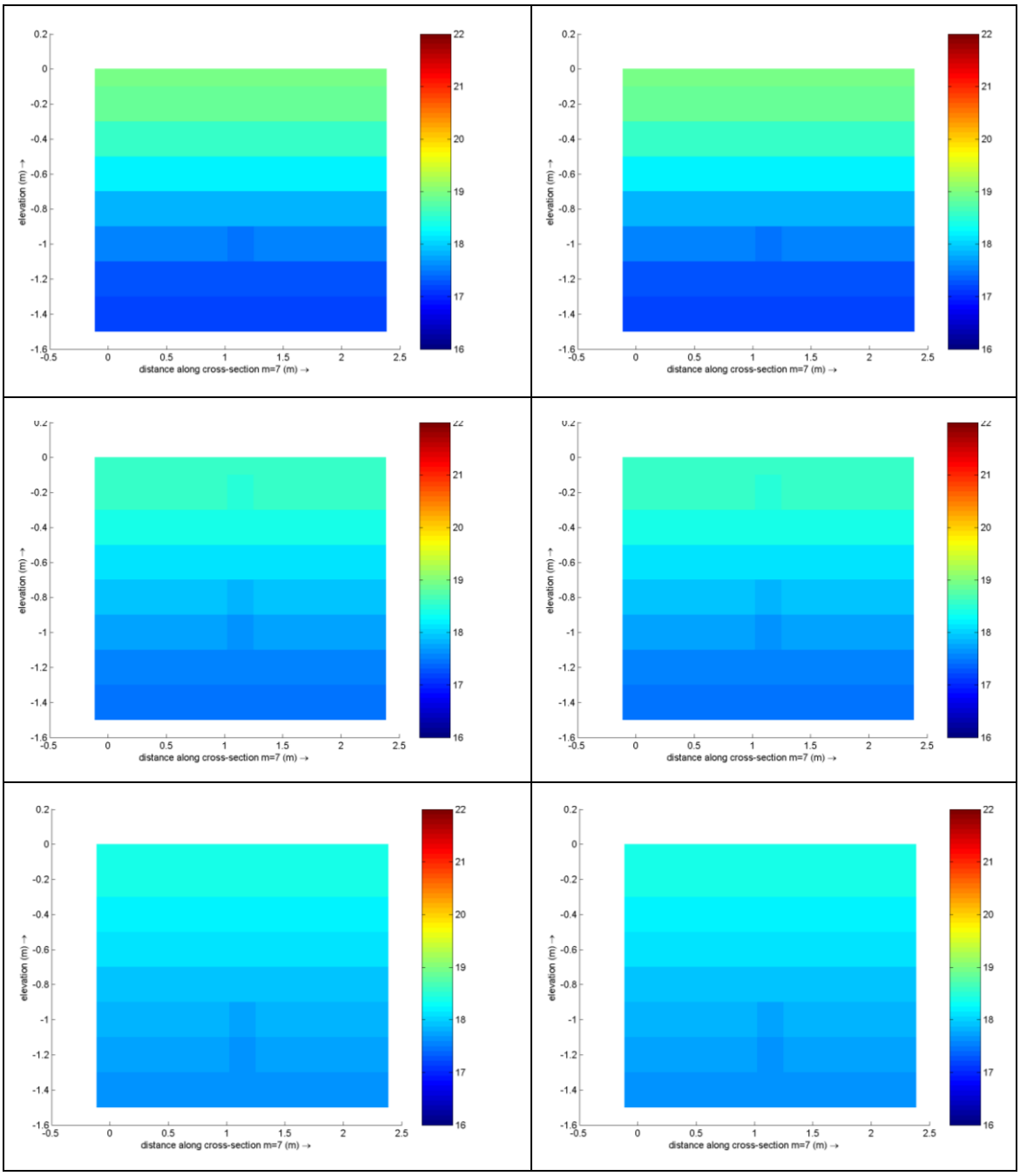
#1	Airlift	8.2
#2	Airlift	7.5
#3	Airlift	8.2
#4	Airlift	10
#5	Airlift	6.5
#6	Airlift	8
#7	Airlift	6.8
#8	Airlift	7

Table B1: All mixing times (in minutes) recorded during the lab experiment.

APPENDIX C: RESULTS SCHEMATISATION EXPERIMENT

Table 5: The results from the schematisations of the experiment with the bubble plume and the airlift from t = 0 to t = 5 min.

Schematisation bubble plume experiment	Schematisation airlift experiment
	
	
	


elevation (m) →
distance along cross-section m=7 (m) →

APPENDIX D: SET-UP DETAILS OF THE DELFT3D SCHEMATISATIONS

D.1 SET-UP DETAILS SCHEMATISATION EXPERIMENT WITH THE BUBBLE PLUME

Domain

Grid: rectangular grid with M = N = 11 (Δm = Δn = 0.23 m) and 8 Z-layers of 12.5% each; this is sufficient to show the mixing of a stratified system.

Bathymetry: uniform 1.5 m below reference level.

Time frame

From 01 Jan 2015 00:00:00 till 01 Jan 2015 00:15:00 (15 min).

Time step: 0.0001 min (0.006 s). The model takes twenty-two seconds to run on an Intel Core2 Duo T9600 processor.

Initial conditions

Uniform water level: h = 0 m.

Temperature per layer from bottom to top: 15, 15, 15, 15, 15, 20, 20, 20 °C.

Boundary conditions

No additional boundary conditions.

Processes

Temperature only.

Physical parameters

Constants: g = 9.81 m/s^2, salinity = 0 ppt.

Bottom roughness: Chezy uniform 65 m$^{1/2}$/s; a smooth wall.

Wall roughness: Partial slip, $L_{roughness}$ = 0.001 m.

Background horizontal eddy viscosity: 1 m^2/s, diffusivity: 1 m^2/s.

Background vertical eddy viscosity: 10^{-6} m^2/s, diffusivity: 10^{-3} m^2/s.

Model for 3D turbulence: k-ϵ; the standard model for turbulence to simulate turbulent flow, using the turbulent kinetic energy *k* and the rate of dissipation of the turbulent kinetic energy *ϵ*.

No heat flux model.

Numerical parameters

Advection scheme for momentum and transport: MDUE; the Delft3D standard for use in Z-layer schematisations.

Bubble plume

The bubble plume is modelled through the additional parameter *filbub*. Its location is in the centre bottom cell (7,7,1) at $z = -1.45\ m$ and the entrained water flow is $Q_{ent} = (\alpha Q_{air})^{0.66} = 40\ l/s$, given that $Q_{air} = 1000\ l/h$ and $\alpha = 27.5$.

D.2 SET-UP DETAILS SCHEMATISATION EXPERIMENT WITH THE AIRLIFT

Domain

Grid: rectangular grid with M = N = 11 (Δm = Δn = 0.23 m) and 8 Z-layers of 12.5% each.

Bathymetry: uniform 1.5 m below reference level.

Time frame

From 01 Jan 2015 00:00:00 till 01 Jan 2015 00:15:00 (15 min).

Time step: 0.0001 min (0.006 s). The model takes twenty-two seconds to run on an Intel Core2 Duo T9600 processor.

Initial conditions

Uniform water level: h = 0 m.

Temperature per layer from bottom to top: 15, 15, 15, 15, 15, 20, 20, 20 °C.

Boundary conditions

No additional boundary conditions.

Processes

Temperature only.

Physical parameters

Constants: g = 9.81 m/s^2, salinity = 0 ppt.

Bottom roughness: Chezy uniform 65 $m^{1/2}/s$

Wall roughness: Partial slip, $L_{roughness}$ = 0.001 m.

Background horizontal eddy viscosity: 1 m^2/s, diffusivity: 1 m^2/s.

Background vertical eddy viscosity: 10^{-6} m^2/s, diffusivity: 10^{-3} m^2/s.

Model for 3D turbulence: k-ϵ.

No heat flux model.

Numerical parameters

Advection scheme for momentum and transport: MDUE; the Delft3D standard for use in Z-layer schematisations.

Airlift

The airlift is modelled as four in-out type discharges. At the location of the airlift, the depth in the bathymetry file is edited to comprise only the top layer. The outlet location of all four is the cell on top of this 'tower' (7,7,1). The inlet locations are the four adjacent bottom cells ((7,6,1), (6,7,1), (7,8,1), (8,7,1)). They have a flow of 10 L/s per discharge. This tower is considered to be small enough to not have a great influence on the water volume and bed friction. Figure 24 shows a cross-section.

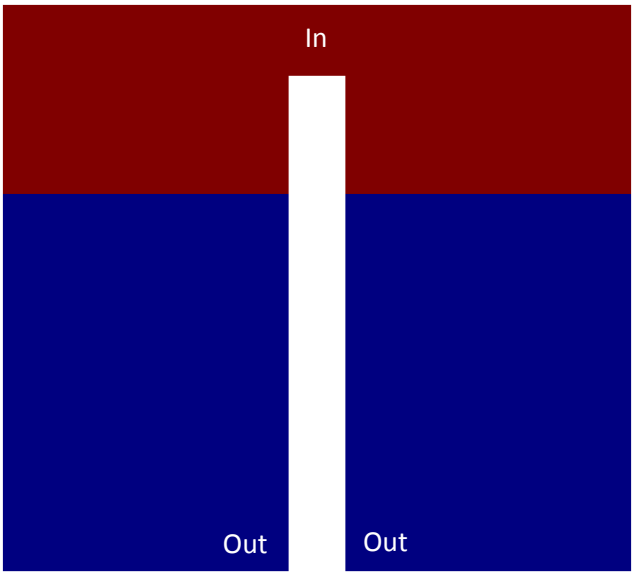


Figure 24: Cross-section of the experiment with edited bathymetry for the airlift.

D.3 SET-UP DETAILS SCHEMATISATION CASE STUDY LAKE *HAARLEMMERMEERSE BOS*

Domain

The lake is gridded as rectangular grid with M = 12 and N = 18 (Δm = Δn = 40 m) and 9 Z-layers (from bottom to top: 19.5% 16% 13% 10.5% 9% 8% 8% 8% 8%). The bathymetry data is from measurements by Brouwer (July 1992), commissioned by *Hoogheemraadschap van Rijnland*. Brouwer used an echo sounder from about every 15 metres, following transects.

Time frame

The process of lake stratification follows a yearly cycle. The model is run from 01 Jan 2013 00:00:00 till 01 Jan 2014 00:00:00, exactly one year. The automatically chosen explicit numerical schemes (see the numerical parameters below) do not allow a time step smaller than 1.5 min. The model takes about 25 minutes to run on an Intel Core2 Duo T9600 processor.

Initial conditions

The main interest is in the results from spring onwards. Since the model spins up in a few days and the run already starts in January, there is sufficient time to spin up and the initial conditions will not influence the results. The water temperature is approximated based on measurements as 4 °C. The water level is uniform, h = 0 m.

Boundary conditions

Lake *Haarlemmermeerse Bos* is isolated from the surrounding water system. It located in a polder that lies 4-5 metres below sea level. It is known for some local salty seepage flows, but this lake has been dug at a location where this is minimal. On a yearly basis, water board *Rijnland* does not consider the ground water as a source.

Processes

The temperature and wind processes are included in this schematisation.

Physical parameters

The standard values of the physical constants suffice, g = 9.81 m/s^2, salinity = 0 ppt, bottom roughness Chezy uniform 45 $m^{1/2}/s$, free slip. The model for 3D turbulence is the recommended k-ϵ turbulence model, verified for the seasonal evolution of the thermocline (Burchard and Baumert, 1995). The background horizontal eddy viscosity and diffusivity values are minimum values for the turbulence closure model and depend on the grid size, but they also function as calibration parameters. For *Lake Haarlemmermeerse Bos*, a background horizontal eddy viscosity of 1 is needed for the damping of artificial oscillations. A background horizontal eddy diffusivity of 0.05 m^2/s is already sufficient, because the mixing should only occur because of the wind or the mixing systems. In the vertical the diffusivity background value needs to be 0 m^2/s in order to minimise mixing of the pycnocline. A background viscosity value of 10^{-3} m^2/s is needed to damp short oscillations caused by wind forcing.

The 'Ocean' heat model is the most detailed and most suitable heat model. It covers the five heat fluxes (solar radiation, atmospheric radiation, back radiation, convection heat loss and evaporation heat loss) by calculating them using simple weather measurements like cloud cover, relative humidity and air temperature. The incoming radiation is calculated from the location on earth and the date. Parameters used are: Secchi depth 2.2 m, Dalton number 0.0015 and Stanton number 0.00145. The relative humidity, air temperature and fraction cloud coverage data are from the KNMI hourly data. The influence of the wind is also incorporated in the model.

The size of the lake is so small that it justifies the choice of a uniform wind speed and direction. The data are the KNMI hourly data. However, the lake is surrounded by many full-grown trees, even though the lake was originally intended for wind surfing. The size of the open space of

the lake is too small for the wind to gain full strength, so the lower influence of the wind is accounted for by decreasing the wind friction values from 0.00063 (0 m/s) and 0.00723 (100 m/s) to 0.00 (0 m/s) and 0.00660 (100 m/s), see Figure 25.

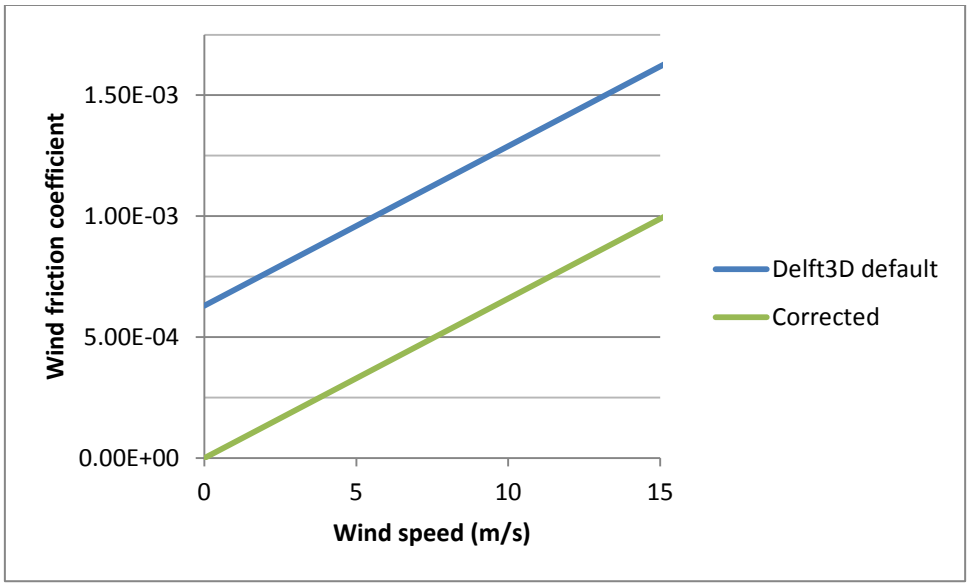


Figure 25 - Wind friction coefficients

Numerical parameters

The drying and flooding checking procedure is left at its default – at grid cell centres and faces – as the water level does not change in this model. The depth in the bathymetry file is specified at the grid cell corners, the depth at the grid cell centres is taken as the mean of the surrounding corner values and the depth at the grid cell faces is the minimum of the two adjacent values.

Because a stratified system is destratified by diffusional processes, the choice of the numerical scheme should be based on numerical diffusivity. Choosing otherwise results in non-physical results, i.e. a fully mixed system while there is no mixing incentive. For horizontal advection of momentum this is the MDUE scheme (Explicit Multi-Directional Upwind scheme, the default option). This scheme couples automatically with the central implicit scheme for vertical advection of momentum to reduce instabilities. For the horizontal advection of transport has been chosen for accuracy again with the Van Leer-2 scheme and for the vertical advection of transport an implicit central scheme (the default options).

Bubble plume

The bubble plumes are modelled through the additional parameter *filbub*. The four locations are (5,5), (5,8), (5,16) and (8,14) at the bottom. These are the locations of the bubble plumes of the current system in lake *Haarlemmermeerse Bos*. The input for the entrained water is 2 m^3/s.

Airlift

The airlift is modelled as four in-out type discharges. No sub-grid calculations are used like in the bubble plume module, all flow properties are handled by the FLOW processor. At the location of the airlift, the depth in the bathymetry file is edited to comprise only the top layer. The outlet location of all four is the cell on top of this 'tower'. The inlet locations are the four cells on the bottom adjacent to this tower. They have a discharge that is a quarter of the discharge per bubble plume. This tower is considered to be small enough to not have a great influence on the water volume and bed friction.

APPENDIX E: MAP OF LAKE *HAARLEMMERMEERSE BOS*



Figure 26 – Location of the measurement location (the dot) and the cross-section used for the results presented in the case study Lake *Haarlemmermeerse Bos*. (Map source: Google Earth.)

APPENDIX F: CALIBRATION OF CASE STUDY LAKE *HAARLEMMERMEERSE BOS*

A calibration is needed for Delft3D to show good results. Several parameters are available for calibration. Specifically for this problem, it is important to calibrate what the influence of turbulent eddies is, because destratification is about adding extra turbulence.

Viscosity

The 3D non-linear shallow water equations in Delft3D are capable of resolving the turbulent scales, but the grid size is too large to resolve fluctuations (Deltares, 2011a). For the momentum equations, therefore Reynolds-averaging is applied (Reynolds, 1894). This introduces Reynolds stresses that are formulated as flow properties multiplied by the horizontal viscosity coefficient ν_H, see equation F.1 and F.2 below. This coefficient is partly a calculated value by the 3D turbulence closure model ($\nu_{3D\ turb.\ cl.\ model}$) and partly user-defined to account for mixing that is not accounted for by the turbulence closure model (ν_H^{back} and ν_V^{back}). (More information on the numerical modelling in Deltares, 2011a and Rodi, 1984).

$$\nu_H = \nu_V + \nu_H^{back} \tag{F.1}$$

$$\nu_V = \nu_{molecular} + \max\left(\nu_V^{back}, \nu_{3D\ turb.\ cl.\ model}\right) \tag{F.2}$$

The background horizontal viscosity coefficient ν_H^{back} represents horizontal turbulence. The vertical turbulence is represented by a combined contribution of the molecular viscosity $\nu_{molecular}$, the background vertical viscosity coefficient ν_V^{back} and the above mentioned factor calculated by the turbulence closure model $\nu_{3D\ turb.\ cl.\ model}$.

The coefficients are velocity scale and length scale dependent and are thus different in every schematisation. They are an-isotropic, which means that the horizontal coefficient exceeds the value of the vertical coefficient ($\nu_H > \nu_V$).

In the schematisation of Lake *Haarlemmermeerse Bos*, the effect of these parameters is the following:

- A higher background horizontal viscosity coefficient ν_H^{back}increases damping of short oscillations. The resulting decrease in vertical mixing keeps the hypolimnion temperature low.

- A higher background vertical viscosity coefficient ν_V^{back} increases the damping of short oscillations. The resulting decrease in vertical mixing decreases the temperature in the metalimnion and hypolimnion.

Diffusivity

The transport of heat is modelled by Delft3D using an advection-diffusion equation in three directions with source and sink terms (Deltares, 2011a). This equation contains a horizontal viscosity coefficient D_H, see equation F.3 and F.4 below. Like for the viscosity coefficient mentioned above, this coefficient is partly a calculated value by the 3D turbulence closure model ($D_{3D\ turb.\ cl.\ model}$) and partly user-defined to account for mixing that is not accounted for by the turbulence closure model (D_H^{back} and D_V^{back}).

$$D_H = D_V + D_H^{back} \tag{F.3}$$

$$D_V = \frac{\nu_{molecular}}{\sigma_{molecular}} + max\left(D_{3D\ turb.\ cl.\ model}\ ,\ D_V^{back} \right) \tag{F.4}$$

The background horizontal diffusivity coefficient D_H^{back} represents horizontal diffusion. The vertical diffusion is represented by a combined contribution of the molecular viscosity $\nu_{molecular}$, the molecular Prandtl number $\sigma_{molecular}$, the background vertical viscosity coefficient D_V^{back} and the factor calculated by the turbulence closure model $D_{3D\ turb.\ cl.\ model}$. The eddy diffusivity is an-isotropic property too ($D_H > D_V$). (Note that if modelling a different constituent than heat, $\sigma_{molecular}$ represents the Schmidt number for diffusion of dissolved matter.)

In the schematisation of Lake *Haarlemmermeerse Bos*, the effect of these parameters is the following:

- A higher background horizontal diffusion coefficient D_H^{back} increases horizontal mixing by diffusion and decreases the depth of the thermocline.
- A higher background vertical diffusion coefficient D_V^{back} increases vertical mixing by diffusion and decreases the steepness of the thermocline. It increases the temperature in the metalimnion and hypolimnion.